Accounting for Temperature Effects When Predicting Molecular Weight and Composition Distribution for Gas-Phase Polyethylene Produced Using a Multi-Site Catalyst

Lauren A. Gibson[1], Jennifer P. Aiello[1], Yan Jiang[2], Timothy Boller[2], Kimberley B. McAuley[1]

[1]Department of Chemical Engineering Queen's University

Kingston, Ontario K7L 3N6, Canada

E-mail: kim.mcauley@queensu.ca

[2]ExxonMobil Chemical Company

Baytown Technology & Engineering Complex 5200 Bayway Dr., Baytown, TX 77520, USA

Abstract

A dynamic model is developed for gas-phase ethylene/1-hexene polymerization with a three-site hafnocene catalyst. The model accurately predicts molecular weight and comonomer composition distributions for fifteen lab-scale copolymerization runs performed at different temperatures. The experimental runs used to fit this model were performed at temperatures between 60 and 85 °C. Gas-phase concentrations were measured every 2.7 minutes throughout each run. Predicted chain-length distributions are discretized to aid model development, keeping the number of ordinary differential equations manageable. Kinetic parameters at the reference temperature of 81 °C and activation energies are estimated. Using parameter subset selection techniques, it is determined that 53 of the 60 model parameters should be estimated using the product characterization and reactor data. An additional data set obtained at 85 °C is used for model validation, confirming the predictive power of the model. The proposed model and its parameter estimates will aid selection of operating conditions to achieve targeted polymer properties.

1. Introduction

Polyethylene (PE) is the most widely produced and widely used polymer in the world.[1] PE is used in many commercial applications including toys, adhesives and medical applications. Commercial linear PE is most often a copolymer of ethylene with different concentrations of an α-olefin comonomer such as 1-butene, 1-hexene and 1-octene. PE can be either amorphous or highly crystalline depending on the level of comonomer incorporation. Comonomer incorporation decreases the

This article has been accepted for publication and undergone full peer review but has not been through the copyediting, typesetting, pagination and proofreading process, which may lead to differences between this version and the Version of Record. Please cite this article as doi: 10.1002/mats.202200023.

density and crystallinity of PE, which changes its physical properties and therefore, increases its suitability for a variety of commercial applications.[2]

PE's wide range of properties is a result of the arrangements of monomer molecules along the polymer chains and the molecular weight distribution (MWD), which are influenced by the catalyst used in the copolymerization. Two of the main types of catalysts used for PE production are Ziegler-Natta catalysts and metallocene catalysts.[1-3] Metallocene catalysts are organometallic coordination compounds with a central transition metal, such as Zr or Hf, surrounded by cyclic organic ligands.[1,4] PEs made using metallocene catalysts can be produced with property profiles that are precisely controllable over a wide range of targets. [1-3] Single-site metallocene catalysts tend to produce PE with good mechanical properties, but limited processability due to narrow MWDs and comonomer composition distributions (CCDs).[2,3] Metallocenes with multiple active sites can broaden the MWD and CCD of PE. Multiple active sites can arise due to interactions of a single metallocene with a catalyst support or due to incorporation of chemically different metallocenes onto a common support.[3] Each site on the metallocene catalyst produces its own joint MWD and CCD.[1,2,5,6] Temperature also influences the behaviour of metallocene catalysts. At higher temperatures, β-hydride elimination reactions are intensified, thereby lowering the average molecular weight of the PE.[4] Temperature also influences the relative rates of ethylene and comonomer incorporation[3], therefore, potentially changing the broadness of MWD and CCD. The metallocene catalyst used for copolymerization in this study is a three-site hafnocene catalyst. It is a special catalyst that produces PE with Broad Orthogonal Composition Distribution, which means that comonomer is incorporated predominantly in the high molecular weight chains.[7] The chemistry behind why the catalyst produces PE with this type of distribution is not well understood.[5]

Engineers want to predict the end-use properties, such as tensile strength, toughness and stiffness of PE from reactor operating conditions, such as temperature and reactant partial pressures, to scale up new polymer products, to optimize commercial reactor performance and to select new catalyst systems from a lab-scale reactor. The end-use properties are influenced by the MWD and CCD. Mathematical models are a useful tool to predict these structural properties of PE made with a particular catalyst system, based on the reactor operating conditions.[8]

The main barrier in the development of fundamental mathematical models to predict PE MWD and CCD is determining appropriate values for the large number of kinetic rate constants. This problem is more difficult when the catalyst has multiple types of active sites, each with its own set of kinetic parameters.[8-10] A further complication is that rates of polymerization reactions in gas-phase PE reactors are influenced by partitioning of reactants between the gas phase and the amorphous polymer that surrounds the catalyst sites where copolymerization occurs.[10-12] When the effects of temperature on the copolymerization are accounted for in mathematical models, the influence of temperature on partitioning must be accounted for, as well as the activation energies for the many kinetic parameters.

In complex models with large numbers of parameters, it is often impossible to estimate all the parameters from the available data, especially when the information in the data is limited due to noisy measurements, a small number of data points or correlated experimental settings.[13] Furthermore, some model parameters may have very little effect on the model predictions, which makes them difficult to estimate. Also, the influence of some parameters can be highly correlated with the influence of other parameters, making simultaneous estimation of these parameters difficult. Therefore, modelers often estimate only a subset of the parameters in their models, and either leave the unestimable parameters fixed at their initial guesses or remove the unestimable parameters by a model simplification.[13] It is important to determine which subset of the model parameters should be estimated from the data and which parameters should be held at constant values to prevent overfitting. In the current article, we use the orthogonalization-based parameter-estimability ranking method developed by Yao et al. (2003)[14] and Thompson et al.[15] to rank the PE model parameters from most-estimable to least-estimable. We then rely on a mean-squared-error (MSE) criterion developed by Wu et al. (2011)[13-18] to determine the appropriate number of parameters to estimate from the ranked list. Estimating more parameters from the ranked list reduces bias in the model prediction but, at the same time, increases the prediction variance. Wu's MSE selection criterion balances the bias and variance to determine the optimal number of parameters to estimate from the available data, thereby preventing overfitting. Yao's estimability ranking methods and Wu's MSE-based criterion have been used to aid parameter estimation in many different chemical and biochemical process models, including polymerization models.[e.g., 15,19-26]

Many researchers have modeled ethylene/α-olefin copolymerization systems over the years, but many of these models do not account for temperature effects.[27-38] **Table 1** summarizes the main PE copolymerization modeling contributions in the literature where activation energies were estimated so that temperature effects could be included.

Table 1. Models where kinetic parameters and activation energies were estimated for Ziegler-Natta and metallocene catalysts used to produce PE.

Author	# of Sites	Phase	Description of Work
Xu et. al (2001)[39], Chakravarti and Ray (2001)[40], Chakravarti, Ray, and Zhang (2001)[41]	1 or 2	Gas	Ethylene homopolymerization with a supported zirconocene metallocene catalyst is modeled using a one-site kinetic model. Ethylene copolymerization with a supported zirconocene metallocene catalyst is modeled using a two-site model. Effects of reaction temperature, pressure, and comonomer concentration on kinetics are investigated. Pre-exponential factors and activation energies for site activation, propagation and catalyst deactivation are estimated.
Kou et. al (2005)[19]	2	Gas	Gas-phase ethylene/hexene copolymerization using a two-site silica-supported zirconocene metallocene catalyst is modeled in a semi-batch reactor. Ethylene consumption rate, gas composition, number- and weight-average molecular weight, short-chain branching levels and triad sequence distributions of copolymer are used to estimate activation, propagation, chain-transfer, re-initiation and deactivation kinetic constants and activation energies.
Thompson et. al	5	Gas	Ethylene/butene and ethylene/hexene copolymerization using a heterogeneous Ti-based

(2007, 2009)[8,15]			Ziegler-Natta catalyst is modeled. Reactor operating conditions are used to estimate propagation, chain transfer, β-hydride elimination and re-initiation rate constants and activation energies. The model is used to predict MWD and average copolymer composition.
Ahmadi et. al (2007)[42]	1	Liquid	Slurry homopolymerization of ethylene with a zirconocene metallocene catalyst is modeled. The pre-exponential factors and activation energies for initiation, propagation, transfer-to-monomer, transfer-to-cocatalyst, spontaneous transfer and spontaneous deactivation reactions are estimated using polymer yield and viscosity-average molecular weight data. The model predicts polymerization rate and number- and weight-average molecular weight.
Mehdiabadi et. al (2013)[43]	1	Liquid	Ethylene solution homopolymerization in a semi-batch reactor with a zirconocene metallocene catalyst is modeled. The effects of ethylene concentration, temperature, and MAO (methylaluminoxane) concentration are investigated. Rate constants and activation energies for propagation, catalyst deactivation, chain transfer to monomer and chain transfer to MAO are estimated using ethylene consumption rate and number- and weight-average molecular weight.
Brandão et. al (2017)[44]	1	Liquid	Ethylene/1,9-decadiene solution copolymerization using a single-site constrained geometry Ti-based catalyst in a semi-batch reactor is modelled. Pre-

			exponential factors and activation energies are estimated for activation, propagation, chain-transfer and deactivation reactions using number- and weight-average molecular weights. Model predicts MWD, level of long-chain branching, ethylene feed rate and number- and weight-average molecular weights.
Caldera et. al (2019)[45]	1	Liquid	Copolymerization of ethylene and 1-hexene using a single-site hafnocene metallocene catalyst in solution is modeled. The rate constants and activation energies for propagation, chain-transfer and deactivation reactions are estimated using ethylene uptake and number-average molecular weight. Polymerization rate, number-average molecular weight and average comonomer incorporation are predicted.

The studies in Table 1 used fundamental mathematical models to estimate kinetic rate constants and activation energies in ethylene homopolymerization or copolymerization with metallocene and Ziegler-Natta catalysts.[8,15,19,39-45] Three of the seven studies involved gas-phase polymerization[8,15,19,39-41], while the other four involved solution or slurry polymerization.[42-45] Three studies modeled ethylene homopolymerization[39-43] and five studies modeled copolymerization with ethylene and an α-olefin comonomer.[8,15,19,39-41,44,45]

To our knowledge, no modeling studies have been reported where kinetic parameters and activation energies have been fitted using joint MWD and CCD data. The objectives of the current research are to: *i*) develop a kinetic model to describe ethylene/hexene copolymerization using a hafnocene catalyst at different temperatures, *ii*) estimate kinetic parameters and activation energies using joint MWD and CCD data along with polymerization rate data from a semi-batch lab-scale reactor. This new model builds on the recent study by Aiello et al. who developed a model to predict the joint MWD and CCD for a similar 3-site hafnocene catalyst at 85 ^{o}C.[11] Temperature effects were not

considered. Like Aiello, we account for vapour-liquid equilibrium between the gas phase and amorphous polymer surrounding the catalyst sites using thermodynamic correlations developed by ExxonMobil.[12]

To aid parameter estimation in the proposed model, the influence of temperature on kinetic rate constants for each reaction are modeled using the following version of the Arrhenius equation:

$$k = k_{ref} e^{-\frac{E_a}{R}(\frac{1}{T}-\frac{1}{T_{ref}})} \quad (1)$$

where k_{ref} is the value of the kinetic rate constant at the reference temperature T_{ref}, and E_a is the activation energy.[46-48] In the current study, $T_{ref} = 354.15\ K$ is used because many of the industrial lab-scale experiments available for parameter estimation were conducted at 81°C.

The remainder of this article is organized as follows. First, we describe the data from 16 batch-reactor data sets which are used to support the modeling effort. Next, a kinetic scheme is proposed, and model equations are presented. An estimability analysis is then used to rank the model parameters from most estimable to least estimable and Wu's mean-squared-error (MSE) criterion is used to determine the optimal number of parameters to estimate from the data. The remaining parameters are held fixed at their initial guesses. Parameters are estimated and the resulting model predictions are compared to data used for parameter estimation. Data from additional validation runs are used to test the predictive capability of the model. In future, this model and its parameter estimates will be valuable for simulating reactor operation using new conditions and for selecting conditions to achieve targeted MWD and CCD properties.

2. Available Data and Experimental Set-Up

ExxonMobil provided lab-scale process data for 16 gas-phase ethylene/hexene copolymerization experiments. The temperature and average properties for polymer collected from the reactor at the end of each run are shown in **Table 2**. Copolymerizations were performed in the autoclave reactor, shown in **Figure 1**, at a constant temperature with a salt bed to aid with heat removal and the mixing of solid polymer. All the catalyst was added to the reactor at the beginning of each experimental run. The catalyst used in the experimental runs is a 3-site hafnocene catalyst that was developed by

ExxonMobil.[7] Ethylene was continuously fed to the reactor to maintain a constant pressure of 2060 kPa_g. A typical ethylene feed rate profile is shown in **Figure 2**. The ethylene feed rate curve has oscillatory behavior due to the tuning of the control system, which is one reason for the low reproducibility of the ethylene feed rate data. Hexene and hydrogen were also fed continuously to the reactor to maintain the ethylene/hexene and ethylene/hydrogen gas-phase ratios near desired targets. Inert gases (isopentane and nitrogen) were added to the reactor to act as gas-phase diluents and to mimic industrial conditions. Gas chromatography (GC) measurements were taken every 2.7 minutes throughout the duration of the experimental runs for use in gas-composition control. The hafnocene catalyst used in these experiments is similar to the catalyst in the modeling study by Aiello et al., except for some changes to the catalyst support material and modifications to the catalyst manufacturing process.

Table 2. Catalyst weight, average polymer properties and reaction temperatures for 16 ethylene/hexene gas-phase experiments conducted with a multi-site supported hafnocene catalyst. Run number 13 is indicated by an asterisk (*) because it was not used for parameter estimation but was saved for model validation.

Run Number	Catalyst Weight (mg)	MI	Grade Density	M_n (g mol^{-1})	M_w	M_z	Avg C6 Wt%	Mass Polymer (g)	Temperature (^oC)
1	16.2	0.406	0.9285	45891	158651	579820	9.04	25	85
2	15.5	0.465	0.9238	45470	157121	511407	9.84	59	85
3	8.7	0.567	0.9227	38139	134680	452104	9.34	49	85
4	5.9	0.861	0.9251	38474	128976	331008	10.94	41	85
5	8.1	0.835	0.9206	39595	123705	263721	8.53	34	85
6	9.8	0.231	0.9390	43673	179840	560321	10.29	56	85
7	17.7	0.423	N/A	45110	149328	331080	8.7	55	85
8	29.9	1.137	N/A	22805	166950	798100	8.72	24	60
9	20.2	0.728	0.9224	34434	133319	420551	8.32	79	81
10	11.5	0.258	0.9447	47633	169605	469472	8.97	45	81
11	8.2	1.113	0.9227	37692	127849	295105	9.52	50	81

12	6.7	1.099	0.9236	36080	126476	304151	8.78	42	81
13*	7.4	0.732	0.9226	32333	133107	375912	8.95	54	81
14	27.8	6.387	0.9413	48772	185211	132484	8.67	76	60
15	7.1	8.908	0.9445	20275	132484	849760	6.67	42	60
16	7.7	1.905	0.9340	27836	137533	497947	9.33	49	70

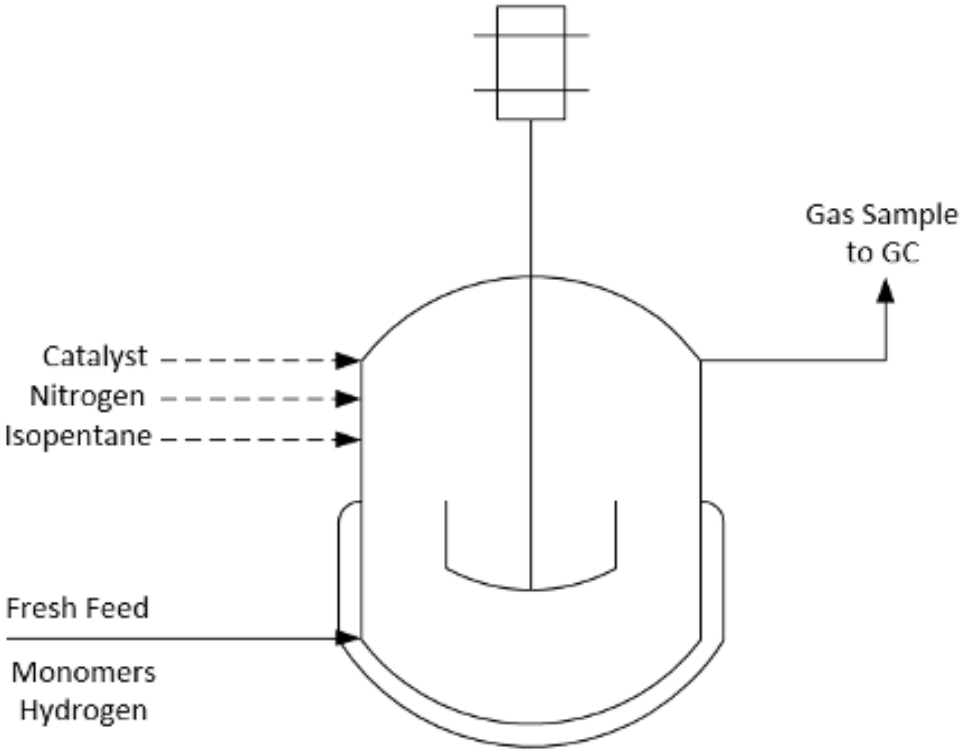

Figure 1. Schematic of the autoclave reactor used for the gas-phase ethylene/hexene copolymerization.[11]

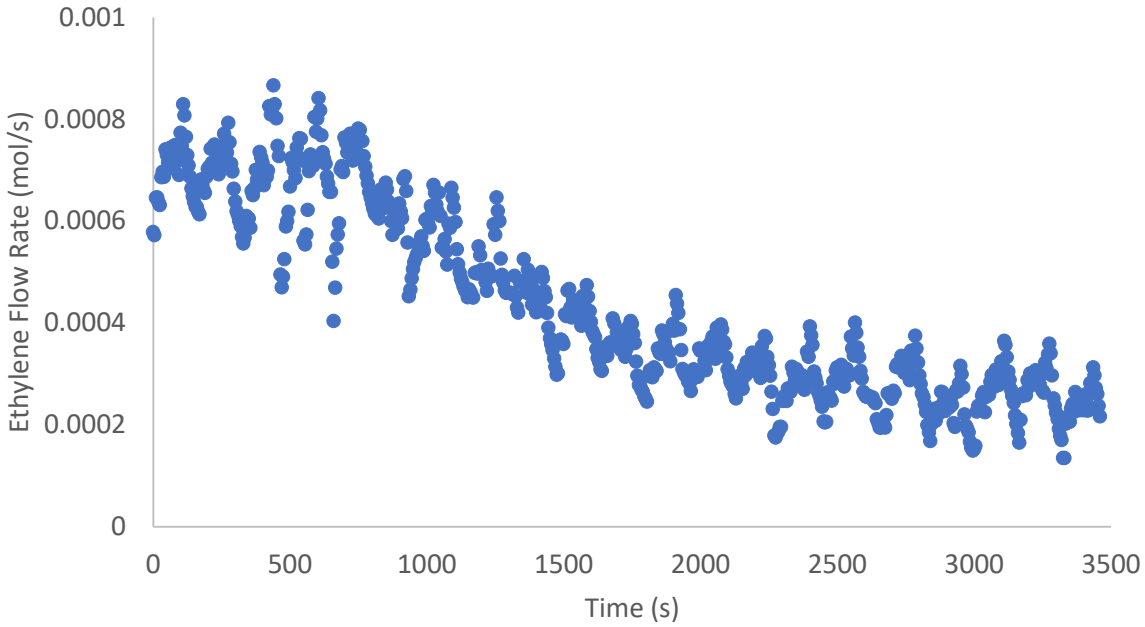

Figure 2. Ethylene feed rate profile for Run #1.

The following measured input data trajectories for each run are available for model development: i) gas-phase concentrations of ethylene, hexene, hydrogen, isopentane and nitrogen, ii) reactor pressure and temperature and iii) ethylene feed rate. After the reaction is complete, the mass of polymer produced was obtained by removing the polymer product from the reactor, separating it from the salt and weighing it. Measurements of the joint MWD and CCD of the final polymer product were obtained using multi-detector Gel Permeation Chromatography (GPC-IR, Polymer Char, Spain) fitted with an IR5 detector. This detector determined the comonomer content of different MWD fractions. The number-average, weight-average and z-average molecular weight were also determined for the final polymer product, along with the overall copolymer composition. Fifteen of the 16 data sets were used for model development while the remaining data set (Run #13) was selected for model validation. This run was selected for validation because it was performed at 81 ^{o}C, the reference temperature. Each data set has 54 data values, so there are 810 data values available for parameter estimation.

The gas-phase composition profiles for Run #1 are shown in **Figure 3**. This run used 16.2 mg of catalyst and produced 25 g of polymer at 85 ^{o}C. Other experimental data for Run #1 is summarized in Table 2. The joint MWD and CCD data for Run #1 are shown in **Figure 4**. All CCDs in this paper have been scaled to protect ExxonMobil confidential industrial data. Figure 4 has two y-axes; the first y-

axis corresponds to the MWD curve in blue, and the second y-axis corresponds to the scaled hexene weight percent in red.

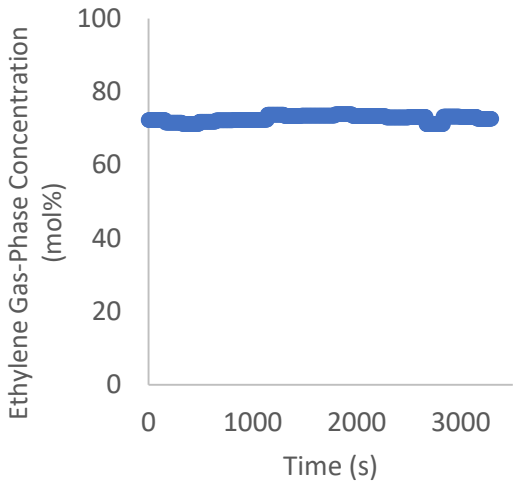

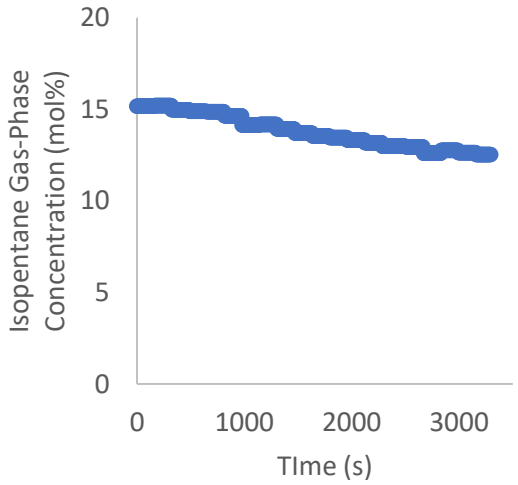

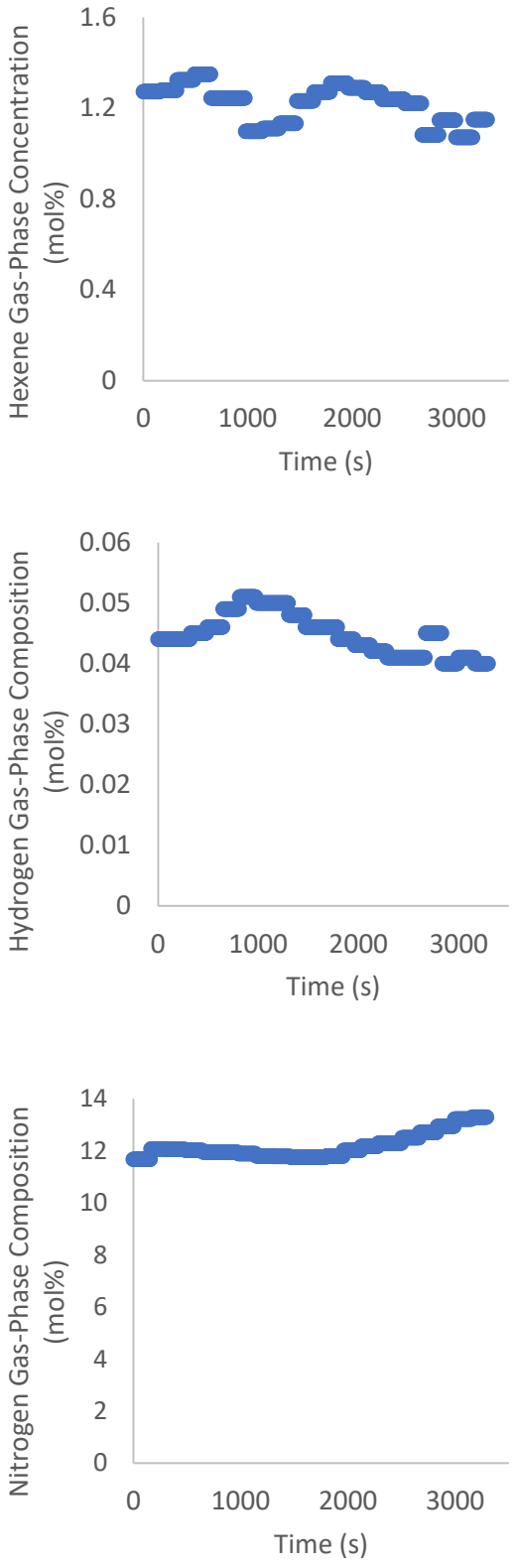

Figure 3. Gas-phase compositions measured during Run #1.

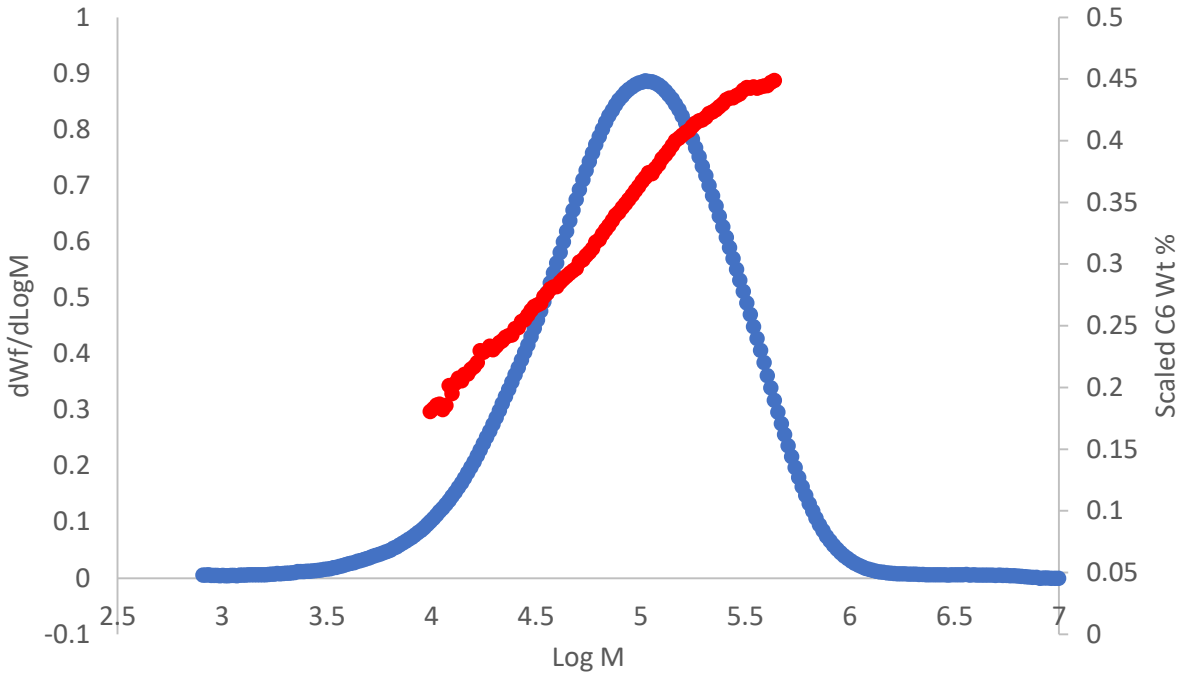

Figure 4. An example of joint MWD and CCD data obtained using GPC-IR. ● MWD, ● comonomer incorporation for corresponding MW fractions.

The raw joint MWD and CCD data from Figure 4 was discretized into bins to aid model development (i.e., to keep the number of ordinary differential equations (ODEs) manageable). Discretizing the raw joint MWD and CCD from Figure 4 into 13 bins with narrow chain length gives the chain-length distribution (CLD) and comonomer fractions in the copolymer shown in **Figure 5**. Details regarding how this discretization was done are found in the Supporting Information. The chain-length bins are sufficiently narrow so that the average molar mass and the average comonomer incorporation within each bin can be assumed constant when converting from MWD to CLD. This assumption and other assumptions used in model development are provided in Table 5. For this catalyst, the chain-length range of interest is 10^2 to $10^{4.6}$ monomeric units. Therefore, the CLD is discretized into 13 equal-width bins from $logr = 2$ to $logr = 4.6$. For example, bin 1 includes the copolymer with chain lengths between $logr = 2$ to $logr = 2.2$ and bin 13 includes the copolymer of chain lengths between $logr = 4.4$ to $logr = 4.6$.

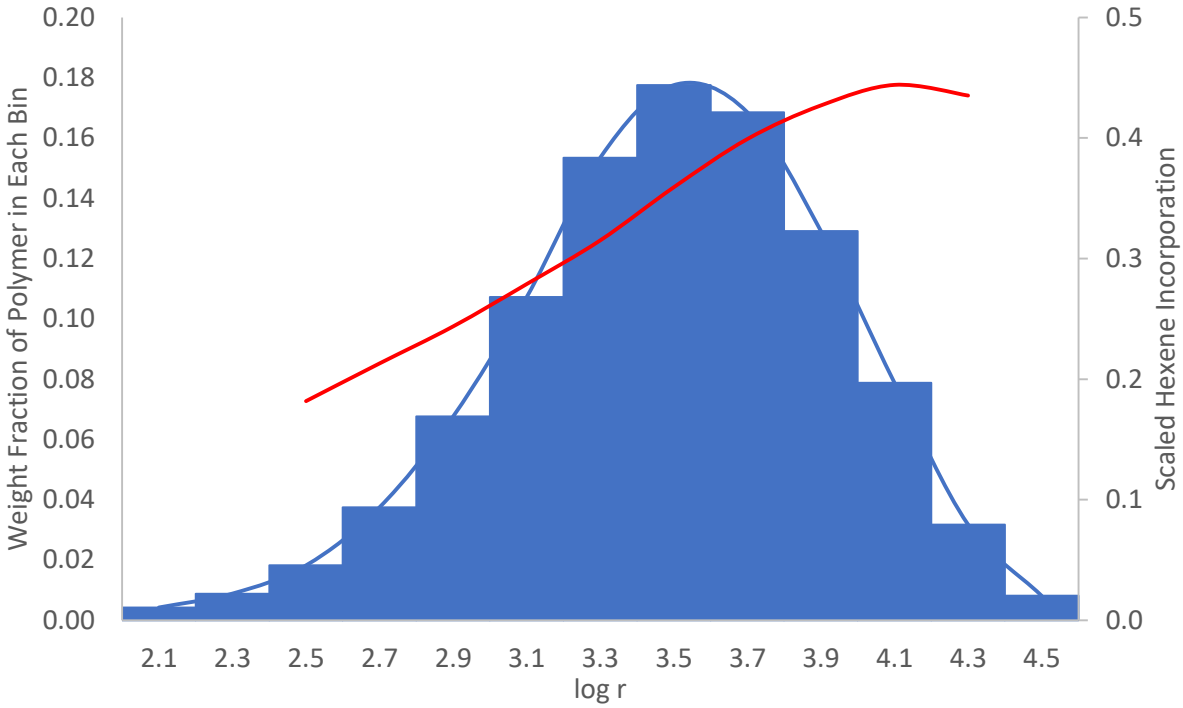

Figure 5. An example of a joint MWD and CCD discretized into 13 bins. — Chain-length distribution, — comonomer incorporation for copolymer in each bin

MWDs for polymer made with a multi-site catalyst are typically modeled as a combination of individual MWDs produced by each catalyst site type.[49,50] The Flory distribution is typically used to model the instantaneous distribution for each site type. Deconvolution studies by ExxonMobil indicated that MWDs produced by the supported hafnocene catalyst in a well-mixed continuous reactor can be approximated by 3 Flory distributions. Therefore, the catalyst used in this study is assumed to have three site types. Site 1 produces copolymer with the lowest average MW and comonomer incorporation, site 3 produces copolymer with the highest MW and comonomer incorporation, and site 2 produces copolymer with intermediate average MW and comonomer incorporation.

2.2 Data Obtained using Different Temperatures

The 16 lab-scale ethylene/hexene copolymerization runs conducted by ExxonMobil have a variety of different reaction temperatures, as summarized in Table 2. Three runs were at 60 °C (Run #8, Run #14, and Run #15), one run was at 70 °C (Run #16), five runs were at 81 °C (T_{ref}) (Run #9 – Run #13) and 7 runs were at 85°C (Run #1 – Run #7). One objective of this study is to estimate the activation energies using joint MWD and CCD data. We are interested in the effect of temperature on the joint MWD and CCD of the polymer because this information will be helpful for development and scale-up of new polymer grades. The discretized joint CLD and CCD for Run #8, which was conducted at 60 °C,

is shown in **Figure 6**. Similarly, the discretized joint CLD and CCD for Run #1 at 85 °C is shown in Figure 5. It is interesting to notice that the CLD (and corresponding MWD) for Run #8 is bimodal. However, the CLD for Run #1 is not bimodal. Also, runs conducted at 60 °C tend to have higher comonomer incorporation, especially in the high MW tail than runs conducted at higher temperatures. So, both MWD and CCD become broader as temperature decreases. This trend occurs because each active site has different activation energies, and therefore produces different curves for the MWD and CCD at different temperatures. Based on the data in Figure 5 and Figure 6, we notice there is relatively more hexene incorporation at low temperatures than at high temperatures. As a result, we believe that site 3 has small activation energies for propagation with hexene.

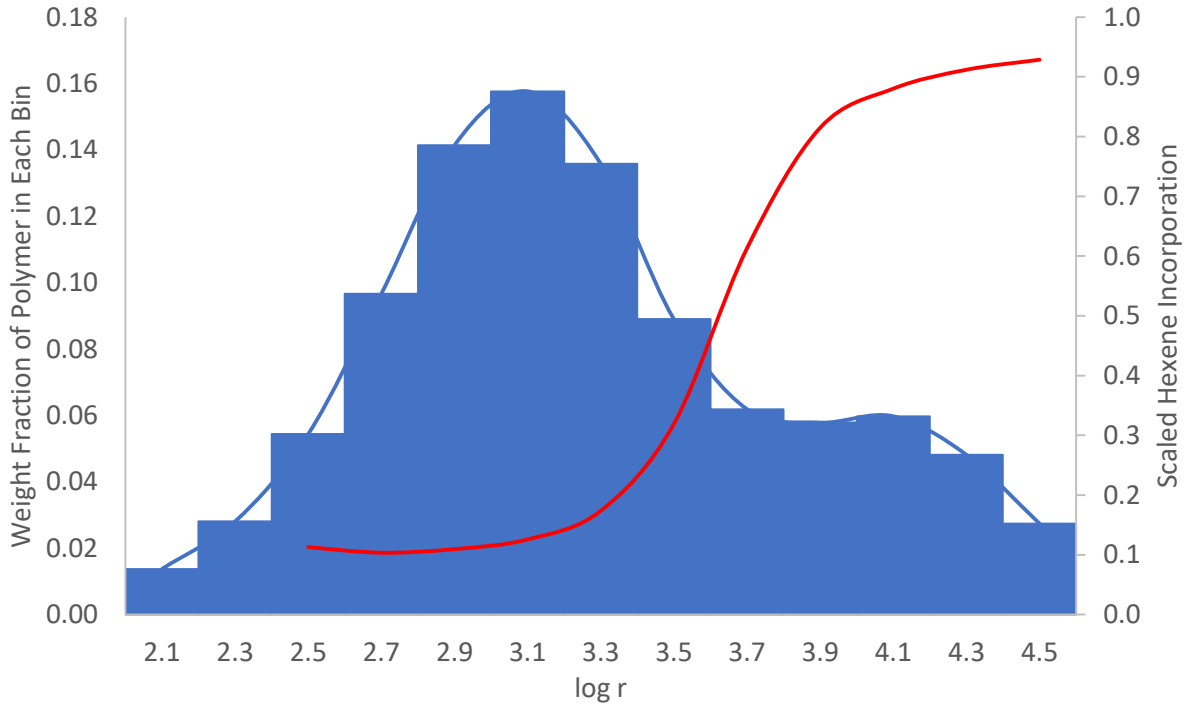

Figure 6. The chain length distribution and corresponding comonomer incorporation for Run #8 at 60°C. — Chain-length distribution, — hexene incorporation distribution as a function of chain length.

2.3 Reproducibility of Experimental Results

The various measurements from the 15 runs for were used for weighted-least-squares parameter estimation based on the following objective function:

$$J = \sum_{d,t} \frac{1}{s_{F_1}^2} (F_{1m} - F_1)^2 + \sum_{d} \frac{1}{s_{m_p}^2} (m_{pm} - m_p)^2 + \sum_{d} \frac{1}{s_{W_2}^2} (W_{2m} - W_2)^2$$

$$+\sum_d \frac{1}{s_{CLD}^2}\sum_{k=1}^{13}(f_{CLDkm}-f_{CLDk})^2+\sum_d \frac{1}{s_{W_{2k}}^2}\sum_{k=1}^{13}(W_{2km}-W_{2k})^2$$

$$+\sum_d \frac{1}{s_{M_n}^2}(M_{nm}-M_n)^2+\sum_d \frac{1}{s_{M_w}^2}(M_{wm}-M_w)^2+\sum_d \frac{1}{s_{M_z}^2}(M_{zm}-M_z)^2 \quad (2)$$

where the subscript m indicates measured values. The summation terms in Equation (2) account for the deviations between measured and predicted values for: ethylene feed rate, mass of polymer produced, average composition of copolymer at the end of the run, weight fraction of polymer in each bin of the discretized CLD, average composition of the copolymer in each bin, number-average molecular weight, weight-average molecular weight, and z-average molecular weight. The index d in the summations refers to the 15 different data sets and the index t refers to 23 measurement times for the ethylene feed rate in each run. The deviations for the weight fraction of polymer in each bin and hexene incorporation in each bin are summed over the 13 bins, $k = 1, \ldots, 13$, for each run. Weighting factors in Equation (2) are required to account for different uncertainties associated with different types of measurement. Values of these weighting factors are provided in **Table 3**. These weighting factors make all terms in the objective function dimensionless. Aiello et al. used replicated experimental runs using a similar 3-site hafnocene catalyst to calculate the standard deviations for each of the responses in Equation (2).[11] The same standard deviations, shown in Table 3, are used for weighted-least-squares parameter estimation in the current study.

Table 3. Measurement errors for experimental data.

Weighting Factor	Measurement Type	Standard Deviation
s_{F_1}	Ethylene Feed Rate [mol s^{-1}]	8.4×10^{-4}
s_{m_p}	Mass of Polymer [kg]	0.016
s_{M_n}	M_n [g mol^{-1}]	4776
s_{M_w}	M_w [g mol^{-1}]	10,583
s_{M_z}	M_z [g mol^{-1}]	215,556
s_{W_2}	Hexene Wt.% in the Final Polymer	0.86
s_{CLD}	Weight Fraction of Polymer in MW Bins #1-13	0.009

$s_{W_{2k}}$	Hexene Wt.% in Bins #1-4, and #10-13	0.9
	Hexene Wt. % in Bins #5-9	0.7

3. Model Development

It is useful to have mathematical models in industry as they aid the development of new commercial products. Accurate kinetic models can predict product properties from reactor operating conditions, thereby reducing the amount of experimental work required for product scale-up.[8,17,51-53] In this study, we develop, fit and validate a kinetic model for ethylene/hexene copolymerization with a three-site supported-hafnocene catalyst using dynamic reactor operating data and copolymer characterization data. This model is designed to provide accurate predictions of joint MWD and CCD for gas-phase ethylene/hexene copolymerization over a wide range of operating conditions (i.e., H_2/C_2 gas-phase mole ratios between 3.8 x 10^{-4} and 6.6 x 10^{-4}, C_6/C_2 gas-phase mole ratios between 0.011 and 0.020 and reactor temperatures between 60 and 85 ^{o}C).

3.1. Kinetic Scheme and Parameters

The proposed kinetic scheme used in the model development is shown in **Table 4**. Reactions in this model include spontaneous activation, propagation with ethylene and hexene, chain transfer to hydrogen, β-hydride elimination and spontaneous deactivation. In this reaction scheme, $S^*(j)$ is a potential active site prior to activation. The index j is used to indicate that there are multiple types of active sites (j = 1, 2 and 3), where each has its own kinetic rate constants. We assumed that each type of catalyst site has the same number of moles of potential active sites per gram of catalyst (see Table 5). The model parameters are estimated based on this somewhat arbitrary assumption. Based on ethylene feed rate data (e.g., see Figure 2), it is apparent that catalyst site activation occurs quickly within the first few minutes of injection into the reactor. As a result, we assume that $k_a(j)$ for j = 1, 2 and 3 is 0.017 s^{-1}, which corresponds to 95% of potential active sites being activated within the first three minutes of the reaction. Setting the value of $k_a(j)$ in this way reduces the number of parameters that require estimation. In Table 4, $N(0,j)$ is an active site of type *j* with chain length zero. $N(0,j)$ can react with ethylene M_1 or hexene M_2 to produce living polymer chains of length $r = 1$. $N(r,j)$, which are growing chains of length r, can react with ethylene or hexene to active sites to produce $N(r+1,j)$.

Chain transfer and deactivation reactions produce dead polymer chains $Q(r)$. Chain transfer to hydrogen H_2 also produces dormant active sites. Since hydrogen does not seem to suppress the overall polymerization rate for this catalyst, it is assumed that dormant active sites, and active sites with chain length zero have the same properties. As such, both are treated as the same species $N(0,j)$ in the model. This assumption, and other assumptions used in model development are summarized in **Table 5**. N_d is a dead catalyst site, which is produced by deactivation reactions. The first 6 assumptions in Table 5 were made by Aiello et. al.[11] in the development of their model. Assumption (1) involving temperature uniformity between the particles and gas phase was justified via heat transfer calculations for this moderate activity catalyst.[54] The last four assumptions are new assumptions used to simplify the parameter estimation and model computations.

Table 4. Proposed kinetic scheme for ethylene/hexene copolymerization with a supported multi-site hafnocene catalyst.

Activation		
(1)	$S^*(j) \xrightarrow{k_a(j)} N(0,j)$	Spontaneous active site formation
Propagation		
(2)	$N(0,j) + M_1 \xrightarrow{k_{p11}(j)} N_1(1,j)\ N(0,j)$	Propagation of an active site with chain length zero with ethylene
(3)	$N(0,j) + M_2 \xrightarrow{k_{p12}(j)} N_2(1,j)$	Propagation of an active site with chain length zero with hexene
(4)	$N_1(r,j) + M_1 \xrightarrow{k_{p11}(j)} N_1(r+1,j)$	Propagation of a terminal ethylene with ethylene
(5)	$N_1(r,j) + M_2 \xrightarrow{k_{p12}(j)} N_2(r+1,j)$	Propagation of a terminal ethylene with hexene
(6)	$N_2(r,j) + M_2 \xrightarrow{k_{p22}(j)} N_2(r+1,j)$	Propagation of a terminal hexene with hexene
(7)	$N_2(r,j) + M_1 \xrightarrow{k_{p21}(j)} N_1(r+1,j)$	Propagation of a terminal hexene with ethylene
Chain Transfer and Elimination		
(8)	$N_1(r,j) + H_2 \xrightarrow{k_{fH1}(j)} N(0,j) + Q(r)$	Chain transfer to hydrogen
(9)	$N_2(r,j) + H_2 \xrightarrow{k_{fH2}(j)} N(0,j) + Q(r)$	Chain transfer to hydrogen

(10)	$N_1(r,j) \xrightarrow{k_{fs1}(j)} N(0,j) + Q(r)$	β-hydride elimination
(11)	$N_2(r,j) \xrightarrow{k_{fs2}(j)} N(0,j) + Q(r)$	β-hydride elimination
Deactivation		
(12)	$N_1(r,j) \xrightarrow{k_{ds1}(j)} N_d + Q(r)$	Spontaneous deactivation
(13)	$N_2(r,j) \xrightarrow{k_{ds2}(j)} N_d + Q(r)$	Spontaneous deactivation
(14)	$N(0,j) \xrightarrow{k_{ds1}(j)} N_d$	Spontaneous deactivation of active site with chain length zero

Table 5. List of assumptions used in model development.

(1)	*Perfect Mixing*: Gas-phase composition and temperature are spatially uniform. Polymer particles are well-mixed. Particles and the gas-phase are at the same temperature.[54] Uniform temperature exists within the particles.
(2)	*Phase Equilibria*: Gas-phase concentrations are in equilibrium with the corresponding amorphous polymer concentrations. Mass-transfer resistances are negligible so the monomer concentrations within the particles are uniform.
(3)	*Terminal Model*: Copolymerization kinetics depend on the type of comonomer at the growing end of the polymer chain and not on the type of comonomer in the penultimate location, nor the length of the polymer chain.
(4)	*Long-Chain Hypothesis*: Monomer is primarily consumed in propagation steps, such that initiation and chain-transfer terms can be neglected in mass balances on monomers.
(5)	*Bin Width*: The chosen bin width is sufficiently narrow so that an average comonomer molecular weight for the monomer/comonomer units within each CLD bin can be used when converting from MWD to CLD.
(6)	*Flory Distributions*: Instantaneous polymer produced by each site type follows a Flory distribution.
(7)	*Active Sites*: Reaction rates for activation do not depend on the concentration of monomers in the reaction mixture. 95% of potential active sites are spontaneously activated in the first 3 minutes. Therefore, the activation rate constant for all sites is $k_a(j) = 0.017\ s^{-1}$ for $j = 1,2,3$.
(8)	*Number of Active Sites:* Each type of catalyst site has the same number of moles of potential active sites per gram of catalyst prior to the beginning of the experimental run.
(9)	*Sites Generated by Chain Transfer to Hydrogen:* The propagation rate constants for

	temporarily-dormant sites are assumed to be the same as the corresponding propagation rate constant for living polymer chains. Therefore, dormant sites and newly activated sites with chain length zero are considered as the same species in our model ($N(0,j)$ for $j = 1,2,3$).
(10)	*Stationary State Hypothesis for* $N(0,j)$: The rate of formation of active sites with chain length zero is assumed to be equal to the rate of consumption of active sites with chain length zero so that ODEs (6.9-6.11) simplify to algebraic equations (6.12-6.14).

3.2. Model Equations

A three-site dynamic model for the semi-batch ethylene/hexene copolymerization using the supported hafnocene catalyst was developed based on the kinetic scheme in Table 4. The model consists of 36 ODEs and 6 algebraic equations shown in **Table 6**, 26 ODEs in **Table 7** and 11 algebraic equations shown in **Table 8**. The ODEs and algebraic equations in Table 6 are material balances. Equations (6.15 – 6.42), which are used to calculate Mn, Mw, and Mz, were obtained using the method of moments.[55] Equation (6.1) is a balance on the total mass of polymer m_p produced in the reactor (in kg). Equation (6.2) is a balance on the mass of hexene m_{2p} consumed in the polymer (in kg). Equations $(6.3 - 6.5)$ are material balance on the number of moles of potential sites in the amorphous polymer at catalyst sites $j = 1, 2$ and 3, respectively. The activation rate constants, $k_a(j)$, are assumed known, so the integrated version of Equations $(6.3 - 6.5)$ are used in the model (see Equations $(6.6 - 6.8)$). Equations $(6.9 - 6.11)$ are material balances on the number of moles of active sites with chain length zero for $j = 1,2$ and 3, respectively. These equations are simplified to Equations $(6.12 - 6.14)$ using the stationary state hypothesis (Assumption 9 in Table 5). Equations $(6.15 - 6.17)$ are balances on the number of moles of growing polymer chains with terminal ethylene at each site type (i.e., on the zeroth moments $Y_1^0(j)$ of the CLD for sites $j = 1,2$ and 3, respectively). Equations (6.18) to (6.26) are the balances on the first, second, and third moments of the CLDs for growing polymer chains *with terminal ethylene* at each of the three types of active sites. Equations (6.27) to (6.38) are balances on the zeroth, first, second, and third moments of the CLDs for growing polymer chains *with terminal hexene* at each of the three types of active sites. Equations $(6.39 - 6.42)$ are balances on the n^{th} moment of the dead polymer CLDs for $n = 0, 1, 2$, and 3 at sites $j = 1, 2$ and 3.

In this model, the moment balances are used to compute average properties of the copolymer (i.e., the number-average molecular weight M_n, the weight-average molecular weight M_w and the z-

average molecular weight M_z). The zeroth-order moments for the living polymer are also used to calculate propagation rates.

Table 6. Mass balance equations for the number of potential active sites and moments of CLD

Balance on the Mass of Copolymer Produced

$$\frac{dm_p}{dt} = \sum_{j=1}^{3}(\{k_{p11}(j)[M_1]MW_1 + k_{p12}(j)[M_2]MW_2\}Y_1^0(j) + \{k_{p21}(j)[M_1]MW_1 + k_{p22}(j)[M_2]MW_2\}Y_2^0(j)) \quad (6.1)$$

Balance on the Mass of Hexene Consumed in Copolymer

$$\frac{dm_{2p}}{dt} = \sum_{i=1}^{3}(k_{p12}(j)[M_2]MW_2Y_1^0(j) + k_{p22}(j)[M_2]MW_2Y_2^0(j)) \quad (6.2)$$

Balance on the Number of Moles of Potential Sites in the Amorphous Polymer

$$\frac{dS^*(j)}{dt} = -k_a(j)S^*(j) \quad (6.3-6.5)$$

Analytical Solution of Equations $(6.3-6.5)$:

$$S^*(j) = S_0^*(j)\exp(-k_at) \quad (6.6-6.8)$$

Balance on the Number of Moles of Active Sites with Chain Length Zero

$$\frac{dN(0,j)}{dt} = k_aS^*(j) - \{k_{p11}(j)[M_1] + k_{p12}(j)[M_2] + k_{ds1}(j)\}N(0,j) + \{k_{fH1}(j)[H_2] + k_{fs1}(j)\}Y_1^0(j) + \{k_{fH2}(j)[H_2] + k_{fs2}(j)\}Y_2^0(j) \quad (6.9-6.11)$$

Assuming Stationary State Hypothesis on Active Sites with Chain Length Zero

$$N(0,j) = \frac{k_aS^*(j) + \{k_{fH1}(j)[H_2] + k_{fs1}(j)\}Y_1^0(j) + \{k_{fH2}(j)[H_2] + k_{fs2}(j)\}Y_2^0(j)}{\{k_{p11}(j)[M_1] + k_{p12}(j)[M_2] + k_{ds1}(j)\}} \quad (6.12-6.14)$$

Moments of Living Polymer Chain-Length Distribution:

1. For Chains with Terminal Ethylene

Zeroth-Order Moment Balance

$$\frac{dY_1^0(j)}{dt} = k_{p11}(j)[M_1]N(0,j) + k_{p21}(j)[M_1]Y_2^0(j)$$

$$-\{k_{p12}(j)[M_2] + k_{fH1}(j)[H_2] + k_{fs1}(j) + k_{ds1}(j)\}Y_1^0(j) \qquad (6.15-6.17)$$

First-Order Moment Balance

$$\frac{dY_1^1(j)}{dt} = k_{p11}(j)[M_1]N(0,j) + k_{p11}(j)[M_1]Y_1^0(j)$$

$$+ k_{p21}(j)[M_1]\{Y_2^1(j) + Y_2^0(j)\}$$

$$-\{k_{p12}(j)[M_2] + k_{fH1}(j)[H_2] + k_{fs1}(j) + k_{ds1}(j)\}Y_1^1(j) \qquad (6.18-6.20)$$

Second-Order Moment Balance

$$\frac{dY_1^2(j)}{dt} = k_{p11}(j)[M_1]N(0,j) + k_{p11}(j)[M_1]\{2Y_1^1(j) + Y_1^0(j)\}$$

$$+ k_{p21}(j)[M_1]\{Y_2^2(j) + 2Y_2^1(j) + Y_2^0(j)\}$$

$$-\{k_{p12}(j)[M_2] + k_{fH1}(j)[H_2] + k_{fs1}(j) + k_{ds1}(j)\}Y_1^2(j) \qquad (6.21-6.23)$$

Third-Order Moment Balance

$$dY_1^3(j) = k_{p11}(j)[M_1]N(0,j) + k_{p11}(j)[M_1]\{3Y_1^2(j) + 3Y_1^1(j) + Y_1^0(j)\}$$

$$+ k_{p21}(j)[M_1]\{Y_2^3(j) + 3Y_2^2(j) + 3Y_2^1(j) + Y_2^0(j)\}$$

$$-\{k_{p12}(j)[M_2] + k_{fH1}(j)[H_2] + k_{fs1}(j) + k_{ds1}(j)\}Y_1^3(j) \qquad (6.24-6.26)$$

2. For Chains with Terminal Hexene

Zeroth-Order Moment Balance

$$\frac{dY_2^0(j)}{dt} = k_{p12}(j)[M_2]N(0,j) + k_{p12}(j)[M_2]Y_1^0(j)$$

$$-\{k_{p21}(j)[M_1] + k_{fH2}(j)[H_2] + k_{fs2}(j) + k_{ds2}(j)\}Y_2^0(j) \qquad (6.27-6.29)$$

First-Order Moment Balance

$$\frac{dY_2^1(j)}{dt} = k_{p12}(j)[M_2]N(0,j) + k_{p22}(j)[M_2]Y_2^0(j)$$

$$+ k_{p12}(j)[M_2]\{Y_1^1(j) + Y_1^0(j)\}$$

$$-\{k_{p21}(j)[M_1] + k_{fH2}(j)[H_2] + k_{fs2}(j) + k_{ds2}(j)\}Y_2^1(j) \qquad (6.30-6.32)$$

Second-Order Moment Balance

$$\frac{dY_2^2(j)}{dt} = k_{p12}(j)[M_2]N(0,j) + k_{p22}(j)[M_2]\{2Y_2^1(j) + Y_2^0(j)\}$$
$$+ k_{p12}(j)[M_2]\{Y_1^2(j) + 2Y_1^1(j) + Y_1^0(j)\}$$
$$-\{k_{p21}(j)[M_1] + k_{fH2}(j) + k_{fs2}(j) + k_{ds2}(j)\}Y_2^2(j) \qquad (6.33-6.35)$$

Third-Order Moment Balance

$$\frac{dY_2^3(j)}{dt} = k_{p12}(j)[M_2]N(0,j) + k_{p22}(j)[M_2]\{3Y_2^2(j) + 3Y_2^1(j) + Y_2^0(j)\}$$
$$+ k_{p12}(j)[M_2]\{Y_1^3(j) + 3Y_1^2(j) + 3Y_1^1(j) + Y_1^0(j)\}$$
$$-\{k_{p21}(j)[M_1] + k_{fH2}(j) + k_{fs2}(j) + k_{ds2}(j)\}Y_2^3(j) \qquad (6.36-6.38)$$

Moments of Dead Polymer Chain Length Distribution

$$\frac{dX^n(j)}{dt} = \sum_{3}^{j=1}\{k_{fs1}(j) + k_{fH1}(j)[H_2] + k_{ds1}(j)\}Y_1^n(j)$$
$$+\{k_{fs2}(j) + k_{fH2}(j)[H_2] + k_{ds2}(j)\}Y_2^n(j) \qquad (6.39-6.42)$$

The equations in Table 7 are used to calculate the average MW and CC properties for each of the 13 bins based on instantaneous Flory distributions produced at each site type, which change over time due to changing reactor conditions.[56] Equations $(7.1-7.13)$ are balances on the mass of dead polymer that belongs in the 1st to 13th bin, respectively. $R_p(j)$ is the overall rate of propagation for sites $j = 1,2$ and 3. Equations $(7.14-7.26)$ are balances on the mass of hexene incorporated into the copolymer belonging to the 1st to 13th bins of the discretized MWD. $R_{2p}(j)$ is the rate of propagation with hexene for site type j.

Table 7. Mass balances used to predict the molecular weight and comonomer composition distributions.

Balances on the Mass of Dead Polymer in each MW Bin[11]

$$\frac{\mathrm{d}m_{pk}}{\mathrm{dt}} = \sum_{j=1}^{3} R_p(j)\int_{logr_k}^{logr_{k+1}}\left(\frac{dw(logr,j)}{dlogr}\right)\mathrm{dlogr} \qquad (7.1-7.13)$$

where

$$R_p(j) = \{k_{p11}(j)[M_1]MW_1 + k_{p12}(j)[M_2]MW_2\}Y_1^0(j) + \{k_{p21}(j)[M_1]MW_1 + k_{p22}(j)[M_2]MW_2\}Y_2^0(j)$$

and

$$\int_{logr_k}^{logr_{k+1}} \left(\frac{dw(logr,j)}{dlogr}\right) \mathrm{dlogr} = -\exp(-r_{k+1}\tau(j))\,(r_{k+1}\tau(j)+1) + \exp(-r_k\tau(j))\,(r_k\tau(j)+1)$$

Mass of Hexene Incorporated in each MW Bin[11]

$$\frac{\mathrm{d}m_{2pk}}{\mathrm{dt}} = \sum_{j=1}^{3} R_{p2}(j) \int_{logr_k}^{logr_{k+1}} \left(\frac{dw(logr,j)}{dlogr}\right) \mathrm{dlogr} \qquad (7.14 - 7.26)$$

where

$$R_{p2}(j) = k_{p12}(j)[M_2]MW_2Y_1^0(j) + k_{p22}(j)[M_2]MW_2Y_2^0(j)$$

Algebraic equations in Table 8 are used to calculate polymer properties and monomer solubility information. Equation (8.1) calculates the hexene weight percent in the final polymer product, based on m_p and m_{2p}. Equation (8.2) calculates $\tau(j)$, the ratio of chain-stopping reaction rates to chain-propagation reaction rates. $\tau(j)$ is used in Equations (7.1) to (7.26). Equations (8.3) to (8.5) calculate the number-average molecular weight M_n, weight-average molecular weight M_w, and z-average molecular weight M_z, respectively. The molecular weight averages are calculated using MW_Y, which is the average molar mass of the monomer units in the growing polymer chains.

Similarly, MW_x, is the average molar mass of the monomer units in the dead polymer chains. Equations (8.6) to (8.8) calculate the concentrations of ethylene, hexene and hydrogen in the amorphous phase using partition coefficients. The partition coefficients K_1, K_2 and K_3 are computed using a thermodynamic correlation developed by ExxonMobil.[12] Equation (8.9) calculates the weight fraction of polymer accumulated in the 1st to 13th bins based on the mass of dead polymer m_{pk} in the k^{th} bin and the overall mass of polymer m_p. This equation is used to determine the CLD of the polymer. Equation (8.10) calculates the weight percent of hexene in the copolymer in the 1st to the 13th bin based on m_{2pk}, the mass of hexene incorporated in the copolymer in the k^{th} bin, for k=1..13. Equation (8.11) calculates the ethylene feed rate F_1 required to maintain the reactor pressure, based on the ethylene consumption rate.

Table 8. Algebraic equations used to predict polymer-property and ethylene feed rate data

Hexene Wt% in the Polymer after reaction

$$W_2 = \frac{m_{2p}}{m_p} \times 100\% \tag{8.1}$$

Ratio of chain-stopping reaction rates to chain-propagation reaction rates

$$\tau(j) = \frac{\left(k_{fs1}(j)+k_{fH1}(j)[H_2]+k_{ds1}(j)\right)Y_1^0(j)+\left(k_{fs2}(j)+k_{fH2}(j)[H_2]+k_{ds2}(j)\right)Y_2^0(j)}{\left(k_{p11}(j)[M_1]+k_{p12}(j)[M_2]\right)Y_1^0(j)+\left(k_{p21}(j)[M_1]+k_{p22}(j)[M_2]\right)Y_2^0(j)} \tag{8.2}$$

Average Molecular Weight Properties

M_n, Cumulative Number Average Molecular Weight (kg/mol)

$$M_n = \frac{\sum_{j=1}^{3}\left(Y_1^1(j)+Y_2^1(j)\right)MW_Y + \sum_{j=1}^{3}X^1(j)\,MW_X}{\sum_{j=1}^{3}(Y_1^0(j)+Y_2^0(j)+X^0(j))} \tag{8.3}$$

where

$$MW_Y = \frac{r_{p1}(j)}{r_p(j)}MW_1 + \frac{r_{p2}(j)}{r_p(j)}MW_2$$

$$MW_X = \frac{m_{1p}}{m_p}MW_1 + \frac{m_{2p}}{m_p}MW_2$$

M_w, Cumulative Weight Average Molecular Weight (kg/mol)

$$M_w = \frac{\sum_{j=1}^{3}\left(Y_1^2(j)+Y_2^2(j)\right)MW_Y + \sum_{j=1}^{3}X^2(j)\,MW_X}{\sum_{j=1}^{3}(Y_1^1(j)+Y_2^1(j)+X^1(j))} \tag{8.4}$$

M_z (kg/mol)

$$M_z = \frac{\sum_{j=1}^{3}\left(Y_1^3(j) + Y_2^3(j)\right) MW_Y + \sum_{j=1}^{3} X^3(j)\, MW_X}{\sum_{j=1}^{3}(Y_1^2(j) + Y_2^2(j) + X^2(j))} \quad (8.5)$$

Concentration of Reactants (mol/m^3) in Amorphous Polymer using Partition Coefficients

$$[M_1] = \frac{[M_1]_g}{K_1} \quad (8.6)$$

$$[M_2] = \frac{[M_2]_g}{K_2} \quad (8.7)$$

$$[H_2] = \frac{[H_2]_g}{K_H} \quad (8.8)$$

Weight Fraction of Overall Polymer in each Bin, to obtain the weight CLD

$$f_{CLDk} = \frac{m_{pk}}{m_p} \quad (8.9)$$

Hexene Wt% in Colymer in each Bins, to predict the Comonomer Incorporation Data

$$W_{2k} = \frac{m_{2pk}}{m_{pk}} \times 100\% \quad (8.10)$$

Ethylene Consumption Rate (mol/s)

$$F_1 = k_{p11}(1)[M_1]Y_1^0(1) + k_{p21}(1)[M_1]Y_2^0(1) + k_{p11}(2)[M_1]Y_1^0(2) + k_{p21}(2)[M_1]Y_2^0(2) + k_{p11}(3)[M_1]Y_1^0(3) + k_{p21}(3)[M_1]Y_2^0(3) \quad (8.11)$$

4. Parameter Estimation

The proposed model will be used to provide accurate predictions for polymer properties over a wide range of operating conditions. As a result, accurate values of kinetic parameters k_{ref}, and activation energies E_a are required for each reaction shown in Table 4. There are 30 kinetic parameters involved in the kinetic scheme in Table 4, resulting in 60 unknown parameters that require estimation for the three site types: 30 kinetic parameters at the reference temperature and 30 activation energies.

Aiello et. al. estimated 36 kinetic parameters in a related isothermal model for a similar catalyst based on experiments conducted at 85 °C.[11] Their parameter values were used to determine initial

guesses for the 30 k_{ref} values. To reduce difficulties associated with correlated parameters, Aiello et. al. estimated ratios of kinetic parameters rather than individual parameters. This approach also makes it easier to select appropriate lower and upper bounds.[8,16] We adopt the same approach in the current study. **Table 9** shows the parameter ratios that we estimated along with their initial guesses and lower and upper bounds. All parameters are estimated using the 15 data sets at different temperatures starting from the initial parameter estimates obtained by Aiello et al. at a fixed temperature of 85 ^{o}C (see column 2 in Table 9). An alternative approach would be to estimate kinetic parameters from data at each operating temperature and to then use these values to obtain activation energy estimates. The latter approach was not possible because there is not enough data to estimate rate constants at each of the four temperatures used to conduct experiments. For example, there is only one experimental run at 70 ^{o}C

Unfortunately, no previous studies have been performed to estimate activation energies for hafnocene catalysts like the one we used to obtain the data.[8,15,19,40-46] Therefore, there are no literature values that can be used as initial guesses for the activation energies. The lower and upper bounds of E_a, shown in **Table 10**, were selected somewhat arbitrarily to obtain reasonable reaction rates and polymer properties. The lower bounds were chosen to be 0 as E_a cannot be negative. The upper bounds for E_a were chosen to be 323.9 kJ mol^{-1} so that reaction rates at the highest temperature of 85 ^{o}C can be up to 1000 times faster than at the lowest temperature of 60 ^{o}C. We selected an initial value of 88.34 kJ mol^{-1} for E_a in most of the reactions in the reaction scheme.

It is often impossible to estimate all parameters in complicated models with many parameters as multiple sets of parameter values can lead to similar predictions of the data.[14] A formal estimability analysis was used to determine which of the 60 parameters can and should be estimated based on the 810 data values from the 15 experimental runs described above. First, the parameters were ranked from most-estimable to least-estimable using a sensitivity-based estimability analysis.[14] This method takes into consideration the influences of the parameters on predictions of measured data, uncertainties in the initial parameter guesses, measurement uncertainties of response variables, and correlated effects of the parameters.[14,15] The most-estimable parameters tend to have the largest influence on the model predictions, while the least-estimable parameters have little influence on model predictions or are highly correlated with other more influential parameters.[14]

Parameter ranking was performed for the 60 parameters involved in our model, and the results are shown in Table 9 and Table 10 (column 5). The top-ranked parameter is $\frac{k_{p21ref}(1)}{k_{p11ref}(1)}$, which is the rate constant for propagation of ethylene at a terminal hexene compared to the rate constant for propagation of ethylene at a terminal ethylene at site 1. This result makes sense as this parameter accounts for the influence of hexene on ethylene consumption at site 1, thereby influencing both the MWD and CCD. The second-ranked parameter is $\frac{k_{p11ref}(3)}{k_{p11ref}(2)}$, which is the rate of propagation of ethylene at a terminal ethylene for site 3, compared to site 2. The third-ranked parameter is $\frac{k_{p11ref}(1)}{k_{p11ref}(2)}$, which is the rate of propagation of ethylene at a terminal ethylene for site 1, compared to site 2. These results make sense because they influence how much polymer is produced by the different sites. The lowest ranked parameter is $E_{fs2}(2)$, which is the activation energy for β-hydride elimination with a terminal hexene at site 2. The β-hydride elimination reaction influences the average polymer chain length, but its influence is only important when the concentration of hydrogen (the chain-transfer agent) is very low. It is not surprising that it is difficult to estimate the influence of temperature on the β-hydride elimination reaction using the current data set in which all runs use substantial quantities of hydrogen.

Once the parameters were ranked, a mean-squared-error (MSE) selection criterion was used to determine how many of the parameters should be estimated.[13,16-18] The first step in applying this criterion is minimizing the weighted-least-squares objective function (Equation (2)) using the "lsqnonlin" optimizer in MATLAB. This optimizer uses the trust-region-reflective optimization algorithm. The optimization tolerances, TolX and TolFun, were selected to ensure reliable convergence. First, the top ranked parameter was estimated while keeping all other parameters at their initial guesses. Next, the top two parameters from the ranked list were estimated. This optimizer was used repeatedly until all 60 parameters had been estimated together. The results from this study were used to compute Wu's MSE criterion which determined that the top 53 parameters should be estimated and the remaining unestimable parameters should be kept at their initial values.[13,16-18] Estimates for the 53 parameters are provided in Table 9 and Table 10. Unestimable parameters are indicated by "-" in the final column of Table 9 and Table 10. The seven parameters held at their initial guesses are: $\frac{k_{p21ref}(2)}{k_{p11ref}(2)}$, $E_{ds2}(3)$, $\frac{k_{ds2ref}(2)}{k_{ds1ref}(2)}$, $E_{ds2}(2)$, $\frac{k_{fs2ref}(3)}{kfs1ref(3)}$, $E_{fs2}(3)$, and $E_{fs2}(2)$. Three of the seven parameters are for β-hydride elimination reactions. These parameters are difficult to estimate because of the relatively large concentrations of hydrogen used

in all experimental runs, making chain-transfer-to-hydrogen the dominant mechanism for determining the average chain length of the copolymer produced by each type of site.

The standard deviations for the 53 estimable parameters were calculated and shown in Table S1 in the Supporting Information. We found that estimates for 19 of the 53 parameters are significantly different from zero at the 95% confidence level. More data would be required to obtain additional significant parameter values. Correlation coefficients were also calculated and are shown in Table S2. Only the parameters with correlation coefficients larger than 0.9 or less than -0.9 are shown in the table. Notice that there are high levels of correlation among $\frac{k_{fs1ref}(1)}{k_{p11ref}(1)}\Big/\frac{k_{fs1ref}(2)}{k_{p11ref}(2)}$, $\frac{k_{fs2ref}(1)}{k_{fs1ref}(1)}$, $E_{fs1}(1)$, and $E_{fs2}(1)$ indicating that the data set was not informative enough to elucidate the influence of temperature on β- hydride elimination reactions. If accurate model predictions are required in situations where β- hydride elimination is a dominant chain-stopping reaction, then additional data should be obtained at low hydrogen concentrations to improve these parameter estimates.

Table 9. Estimates for the kinetic parameters.

Parameter	Initial Guess	Lower Bound	Upper Bound	Ranking	Estimates
For Catalyst Site Deactivation (s^{-1} or dimensionless)					
$k_{ds1ref}(2)$	1.46×10^{-4}	2.81×10^{-6}	5.28×10^{-3}	15	7.32×10^{-4}
$\frac{k_{ds2ref}(2)}{k_{ds1ref}(2)}$	1	0	10	56	-
$\frac{k_{ds1ref}(1)}{k_{ds1ref}(2)}$	1	0	50	13	0.49
$\frac{k_{ds1ref}(3)}{k_{ds1ref}(2)}$	1	0	50	9	3.37×10^{-2}
$\frac{k_{ds2ref}(1)}{k_{ds2ref}(2)}$	1	0	50	26	49.99
$\frac{k_{ds2ref}(3)}{k_{ds2ref}(2)}$	1	0	50	47	1.00
For Chain Transfer to Hydrogen ($m_{am}^3 mol^{-1} s^{-1}$ or dimensionless)					

$\frac{k_{fH1ref}(2)}{k_{p11ref}(2)}$	15.12	0	50	16	7.06
$\frac{k_{fH1ref}(1)}{k_{p11ref}(1)} \Big/ \frac{k_{fH1ref}(2)}{k_{p11ref}(2)}$	1.66	1	50	10	2.81
$\frac{k_{fH1ref}(3)}{k_{p11ref}(3)} \Big/ \frac{k_{fH1ref}(2)}{k_{p11ref}(2)}$	0.32	0	1	11	0.17
$\frac{k_{fH2ref}(1)}{k_{fH1ref}(1)}$	1	0	10	28	0.16
$\frac{k_{fH2ref}(2)}{k_{fH1ref}(2)}$	1	0	10	42	4.49
$\frac{k_{fH2ref}(3)}{k_{fH1ref}(3)}$	1	0	10	40	0.57
For Spontaneous Chain Transfer (β-hydride elimination) (s^{-1} or dimensionless)					
$\frac{k_{fs1ref}(2)}{k_{p11ref}(2)}$	4.12×10^{-3}	1.0×10^{-5}	0.1	21	3.11×10^{-2}
$\frac{k_{fs1ref}(1)}{k_{p11ref}(1)} \Big/ \frac{k_{fs1ref}(2)}{k_{p11ref}(2)}$	13.53	1	50	35	1.21
$\frac{k_{fs1ref}(3)}{k_{p11ref}(3)} \Big/ \frac{k_{fs1ref}(2)}{k_{p11ref}(2)}$	1	0	50	17	0.13
$\frac{k_{fs2ref}(1)}{k_{fs1ref}(1)}$	1	0	10	43	1.60
$\frac{k_{fs2ref}(2)}{k_{fs1ref}(2)}$	1	0	100	52	2.96×10^{-3}
$\frac{k_{fs2ref}(3)}{k_{fs1ref}(3)}$	1	0	10	58	-
For Chain Propagation ($m_{am}^3 mol^{-1} s^{-1}$ or dimensionless)					
$k_{p11ref}(2)$	2.14	0	100	6	6.46
$\frac{k_{p11ref}(1)}{k_{p11ref}(2)}$	0.45	0.1	50	3	0.71

$\frac{k_{p11ref}(3)}{k_{p11ref}(2)}$	0.61	0.1	50	2	1.67
$\frac{k_{p12ref}(2)}{k_{p11ref}(2)}$	7.26×10^{-2}	0.01	1	5	0.11
$\frac{k_{p12ref}(1)}{k_{p11ref}(1)} \Big/ \frac{k_{p12ref}(2)}{k_{p11ref}(2)}$	0.30	0	1	23	0.22
$\frac{k_{p12ref}(3)}{k_{p11ref}(3)} \Big/ \frac{k_{p12ref}(2)}{k_{p11ref}(2)}$	2.11	1	50	4	1.68
$\frac{k_{p21ref}(1)}{k_{p11ref}(1)}$	2.05×10^{-2}	0	100	1	1.91
$\frac{k_{p21ref}(2)}{k_{p11ref}(2)}$	4.32	0	10	54	-
$\frac{k_{p21ref}(3)}{k_{p11ref}(3)}$	6.57	0	10	53	2.31×10^{-2}
$\frac{k_{p22ref}(1)}{k_{p12ref}(1)}$	0.1	0	10	30	6.89
$\frac{k_{p22ref}(2)}{k_{p12ref}(2)}$	2.87	0	10	48	6.54
$\frac{k_{p22ref}(3)}{k_{p12ref}(3)}$	0.16	0	10	36	6.87×10^{-5}

Table 10. Estimates for the activation energies.

Parameter	Initial Guess	Lower Bound	Upper Bound	Ranking	Estimates
For Catalyst Site Deactivation (kJ mol^{-1})					
$E_{ds1}(1)$	147.2	0	323.9	38	323.9
$E_{ds1}(2)$	147.2	0	323.9	34	136.3
$E_{ds1}(3)$	147.2	0	323.9	29	64.09
$E_{ds2}(1)$	73.61	0	323.9	41	6.87×10^{-5}
$E_{ds2}(2)$	73.61	0	323.9	57	-
$E_{ds2}(3)$	73.61	0	323.9	55	-
For Chain Transfer to Hydrogen (kJ mol^{-1})					

$E_{fH1}(1)$	88.34	0	323.9	22	8.22×10^{-4}
$E_{fH1}(2)$	88.34	0	323.9	14	180.8
$E_{fH1}(3)$	88.34	0	323.9	20	137.5
$E_{fH2}(1)$	88.34	0	323.9	24	197.6
$E_{fH2}(2)$	88.34	0	323.9	46	323.9
$E_{fH2}(3)$	88.34	0	323.9	45	133.4
For Spontaneous Chain Transfer (β-hydride elimination) (kJ mol^{-1})					
$E_{fs1}(1)$	88.34	0	323.9	33	322.8
$E_{fs1}(2)$	88.34	0	323.9	31	120.7
$E_{fs1}(3)$	88.34	0	323.9	27	2.88×10^{-2}
$E_{fs2}(1)$	88.34	0	323.9	49	147.5
$E_{fs2}(2)$	88.34	0	323.9	60	-
$E_{fs2}(3)$	88.34	0	323.9	59	-
For Chain Propagation (kJ mol^{-1})					
$E_{p11}(1)$	58.89	0	323.9	18	9.49
$E_{p11}(2)$	58.89	0	323.9	8	171.0
$E_{p11}(3)$	58.89	0	323.9	7	78.48
$E_{p12}(1)$	58.89	0	323.9	25	2.26×10^{-4}
$E_{p12}(2)$	58.89	0	323.9	19	140.8
$E_{p12}(3)$	58.89	0	323.9	12	39.28
$E_{p21}(1)$	88.34	0	323.9	32	105.9
$E_{p21}(2)$	88.34	0	323.9	39	3.27
$E_{p21}(3)$	88.34	0	323.9	37	88.63
$E_{p22}(1)$	88.34	0	323.9	50	24.62
$E_{p22}(2)$	88.34	0	323.9	44	323.9
$E_{p22}(3)$	88.34	0	323.9	51	166.8

Parameter estimation was performed by minimizing the value of the objective function in Equation (2). For the 15 data sets used in model development, there are 810 data values available to fit the parameters in the model. As shown in **Figure 7**, the value of the objective function was reduced by 92.7% when 53 of the 60 parameters in the ranked list were estimated (Table 9 and Table 10). The value of the objective function, J, decreased only slightly when more parameters were estimated. This result is consistent with the selection of the top 53 parameters using Wu's MSE-based criterion.

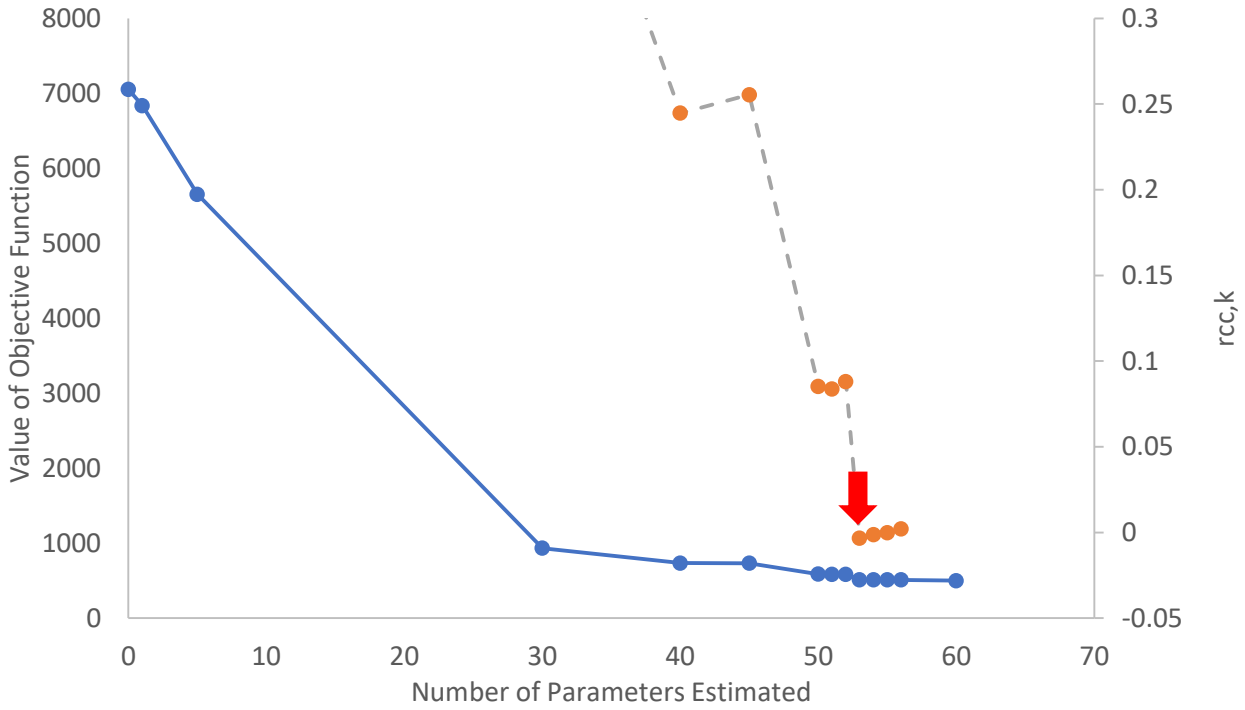

Figure 7. The influence of the number of parameters estimated from the ranked list on the value of the objective function, ●. ●Wu's MSE-based selection criterion $r_{cc,k}$ plotted as a function of the number of parameters estimated. The lowest value of $r_{cc,k}$ occurs when 53 parameters are estimated (shown by the red arrow), indicating that estimating more parameters would result in over-fitting.

5. Simulation Results and Model Validation

The kinetic parameters in Table 9 and Table 10 were used to predict the final polymer properties and ethylene feed rate for all 15 experimental runs used for parameter estimation (see Table 2). Run #12 has the best overall fit to the data out of the 15 runs used for parameter estimation (based on the contribution to the value of the objective function by each data set). Model predictions and data for Run #12, which was conducted at 81 ^{o}C, are compared in **Figure 8**. All the model predictions are

within the error bars for this run. Many of the error bars in Figure 8(c) protrude below the x-axis because the ethylene consumption rate data are not very reproducible from run to run.

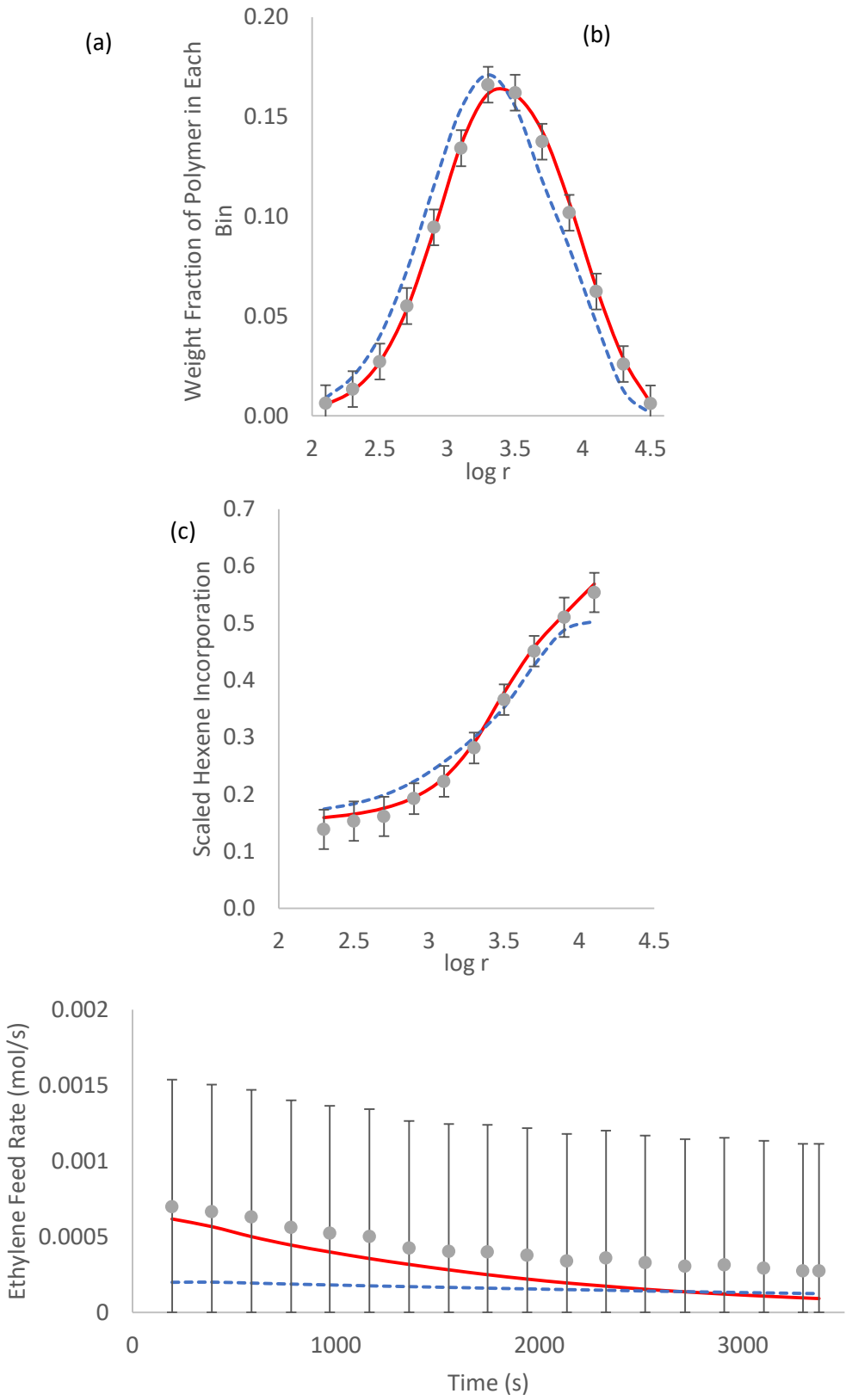

Figure 8. Model fit to data for Run #12 for a) chain length distribution, b) hexene incorporation as a function of chain length, and c) ethylene consumption rate. ● Experimental data, -- predictions

with initial guesses, and — predictions with final estimates from Table 9 and Table 10. Error bars correspond to measurement errors from Table 3.

Figure 9 compares the model predictions and data for Run #6, which has the worst overall fit to the data out of the 15 data sets used for parameter estimation (with the largest contribution to the value of the objective function). The reaction temperature of Run #6 is 85 ^{o}C. The fit to the CLD and ethylene consumption rate data is very good (all predictions within the error bars), but the model underpredicts the amount of hexene incorporated into the polymer. This hard-to-fit run is somewhat unusual in the data set because it has such a high level of measured hexene incorporation. In future, it will be important to perform a replicate experiment to find out whether the experimental results for this run are reproducible. Lastly, **Figure 10** shows the model fit to Run #8, which was conducted at the lowest reaction temperature of 60 ^{o}C. The fit for this run is also acceptable. The corresponding plots for the other 12 runs are provided in the Supplemental Information.

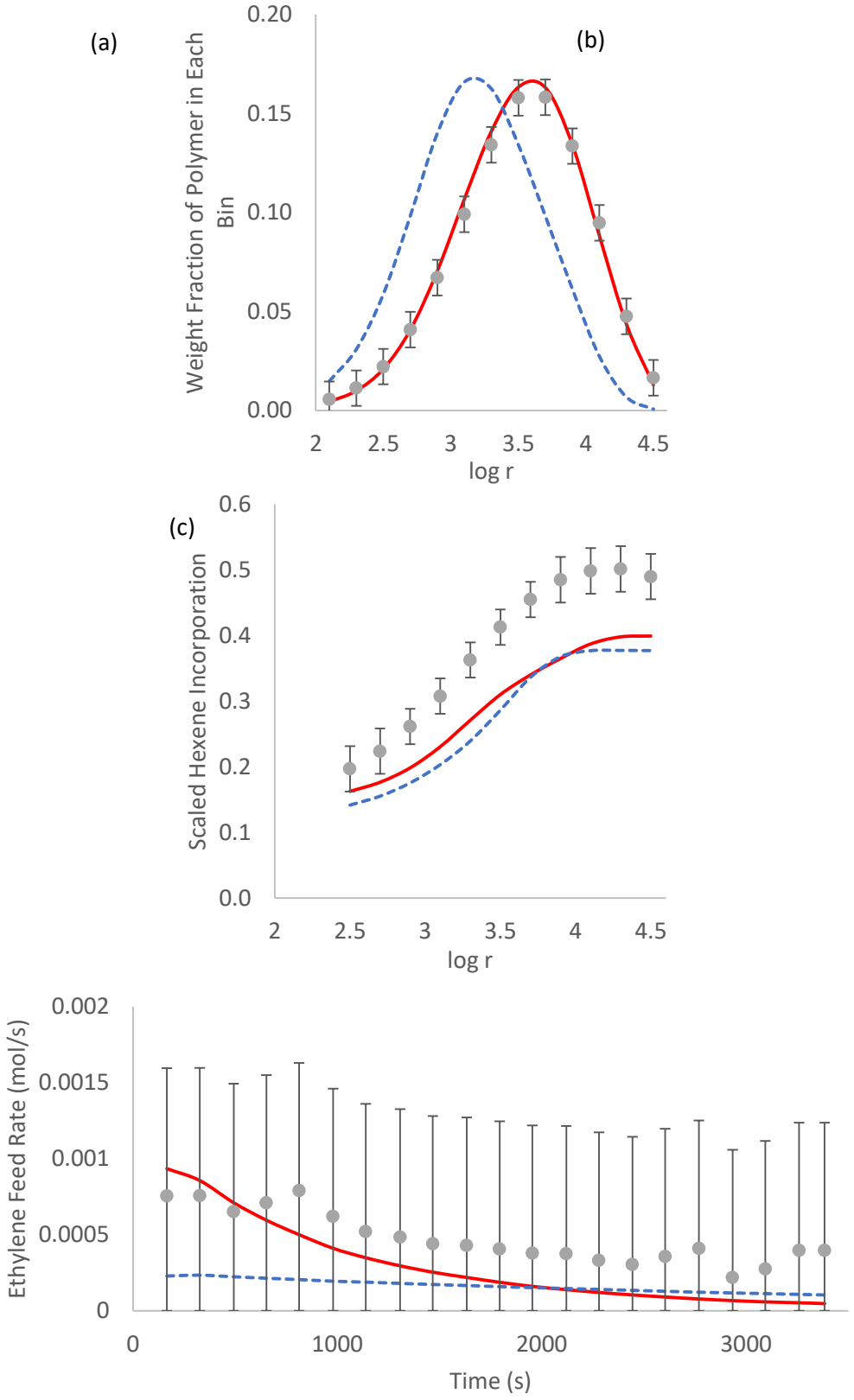

Figure 9. Model fit to data for Run #6 for (a) chain length distribution, (b) hexene incorporation as a function of chain length, and (c) ethylene consumption rate. ● Experimental data, -- predictions with initial guesses, and — predictions with final estimates from Table 9 and Table 10. Error bars correspond to measurement errors from Table 3.

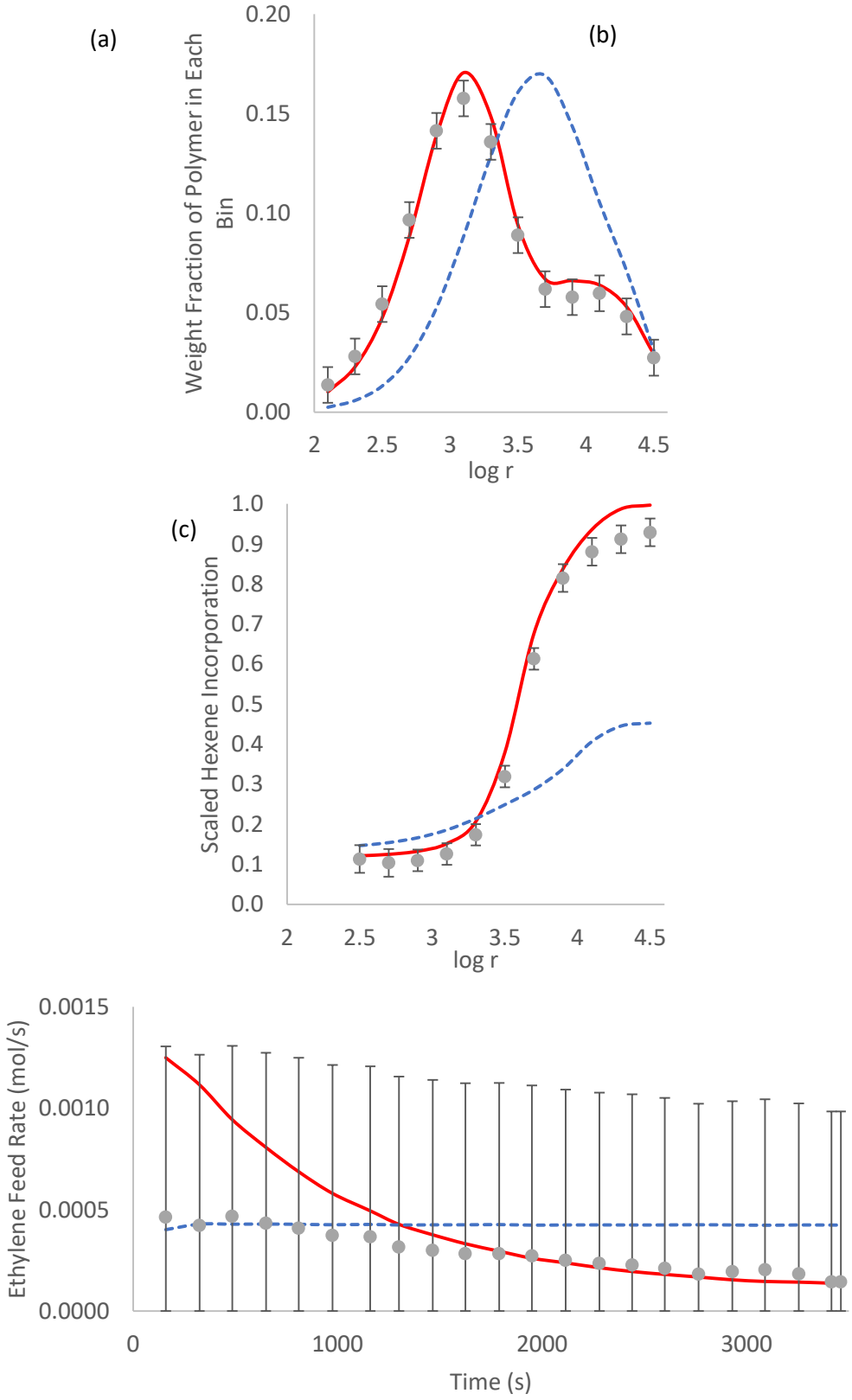

Figure 10. Model fit to data for Run #8 for (a) chain length distribution, (b) hexene incorporation distribution as a function of chain length, and (c) ethylene consumption rate. ● Experimental data, - - -

predictions with initial guesses, and — predictions with final estimates from Table 9. Error bars correspond to measurement errors from Table 3.

One data set (Run #13) was left out of the parameter estimation, so it can be used for model validation. **Figure 11** compares the model predictions to experimental data for this validation run, which was conducted at 81 °C. The CLD, CCD, and ethylene feed rate predictions provide a good match to the data. The model also gives reliable predictions for the mass of polymer produced during Run #13, the overall composition of the copolymer that was produced, and average molecular weights, as shown in **Figure 12**.

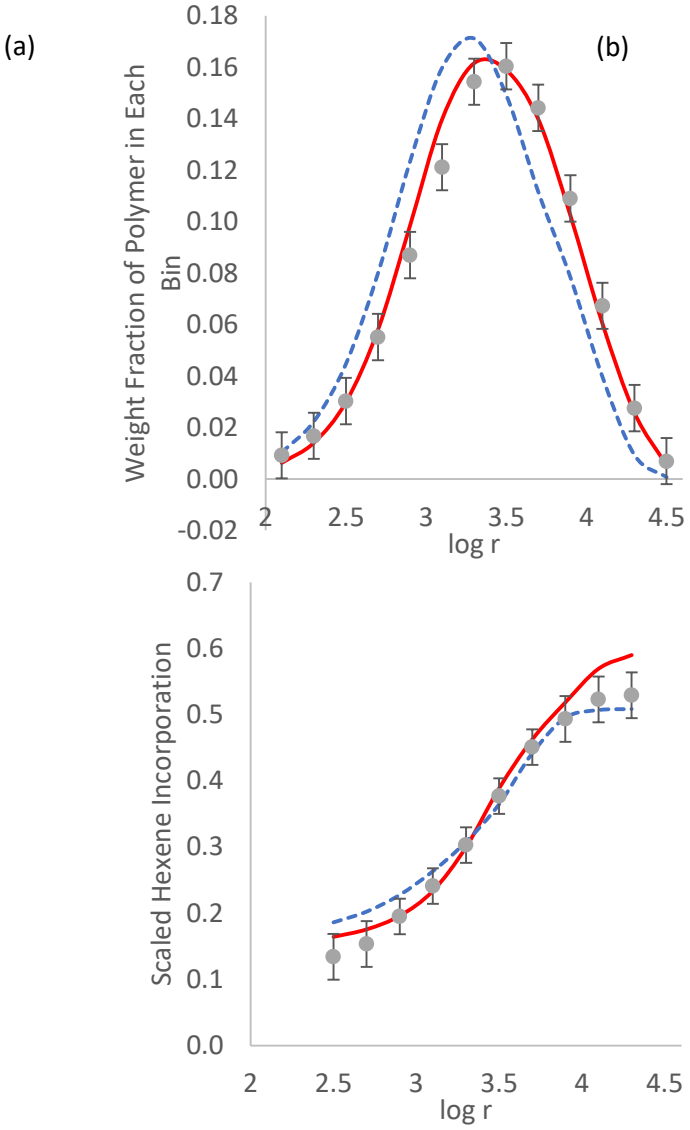

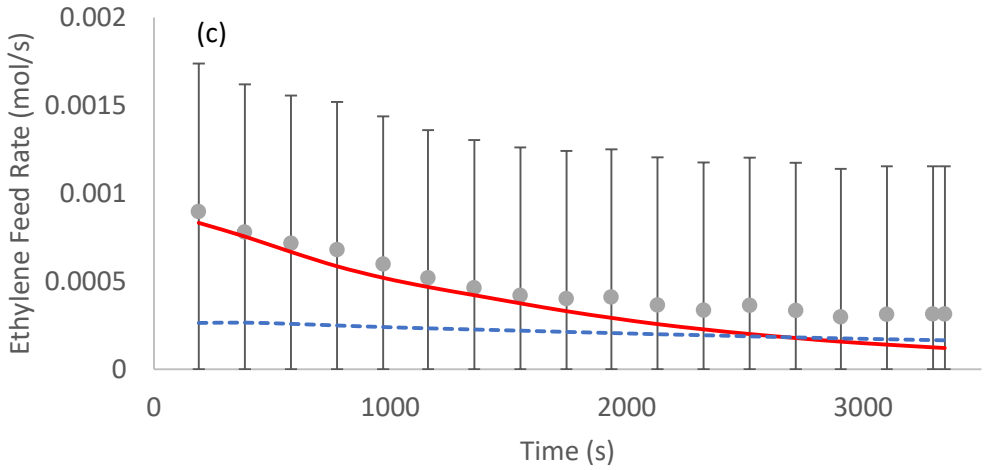

Figure 11. Model fit to data for Run #13 for (a) chain length distribution, (b) hexene incorporation distribution as a function of chain length, and (c) ethylene consumption rate. ● Experimental data, - - predictions with initial guesses, and — predictions with final estimates from Table 9 and Table 10. Error bars correspond to measurement errors from Table 3.

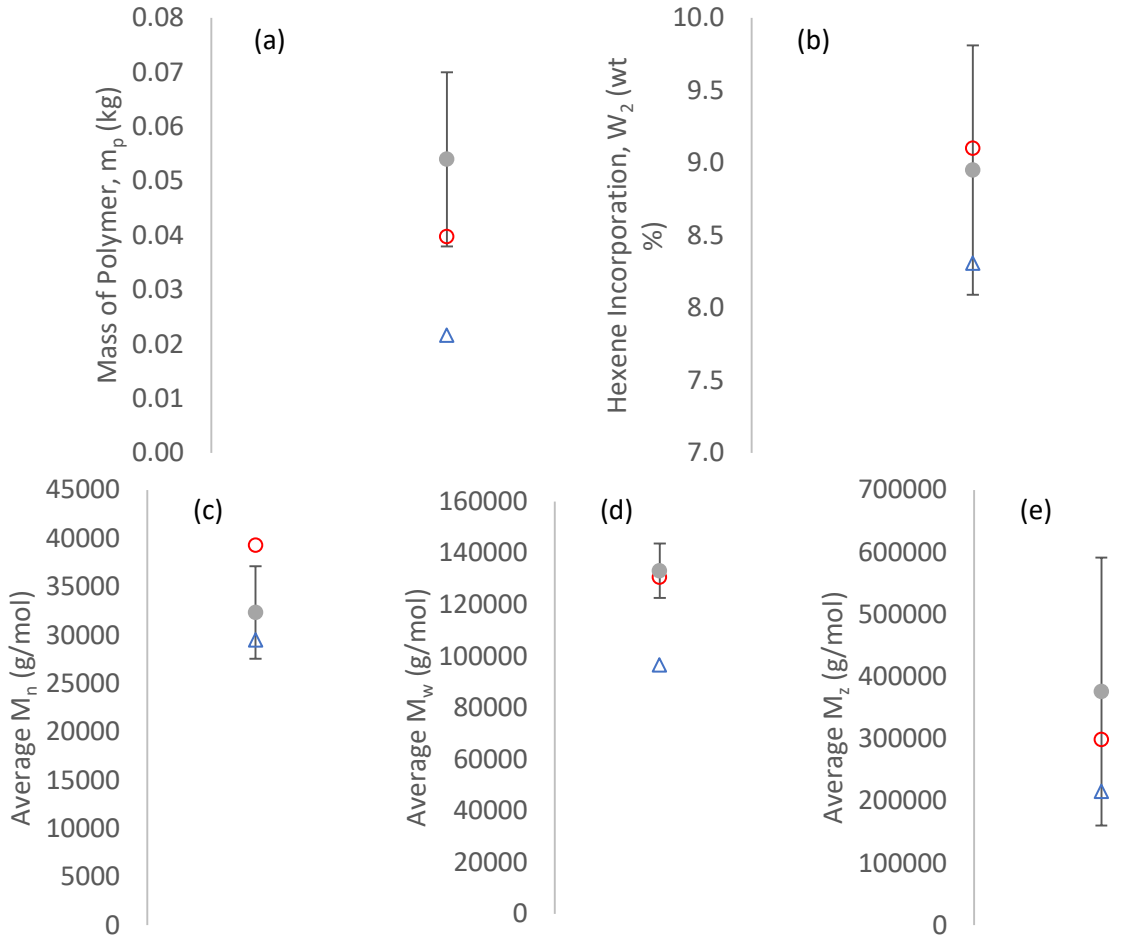

Figure 12. Model predictions for Run #13 for (a) mass of polymer, (b) hexene incorporation in the copolymer, (c) number-average molecular weight, (d) weight-average molecular weight and e) z-average molecular weight. ● Experimental data, △ predictions with initial guesses, and ○ predictions with final estimates from Table 9. Error bars correspond to measurement errors in Table 3.

The model predicts the mass of polymer, hexene incorporation, and weight-average and z-average molecular weights very well (see (a), (b), (d), and (e) in Figure 12) as the predictions fall within the experimental error bars. The model does a reasonable job do of predicting the number-average molecular weight (see (c) in Figure 12) with the predicted value falling just outside of the error bar.

6. Conclusions

A dynamic model was developed for gas-phase ethylene\1-hexene copolymerization with a 3-site hafnocene catalyst to predict the joint chain length and comonomer incorporation distribution over a range of temperatures from 60 to 85 ^{o}C. The model also predicts the ethylene consumption rate,

mass of polymer produced, and average characteristics of the final polymer product (e.g., number-average molecular weight, weight-average molecular weight and average composition).

Fifteen dynamic lab-scale ethylene\1-hexene copolymerization data sets were used to develop the model. The remaining 16th data set was used for model validation. Out of the 15 experimental runs used for model development, 3 have a reaction temperature of 60 ^{o}C, 1 has a reaction temperature of 70 ^{o}C, 4 have a reaction temperature of 81 ^{o}C, and 7 have a reaction temperature of 85 ^{o}C. The kinetic scheme developed for the copolymerization reaction includes spontaneous activation, propagation with ethylene and hexene, chain transfer to hydrogen, β-hydride elimination, and spontaneous deactivation reactions. There are 30 kinetic parameters in the model, so 30 kinetic parameters at the reference temperature of 81 ^{o}C, and 30 activation energies are unknown and must be estimated.

A formal estimability analysis was done to rank the parameters from most-estimable to least-estimable. An MSE-based selection criterion was used to determine that 53 of the 60 parameters should be estimated from the data. The data from the validation run at 81 ^{o}C was used to assess the predictive ability of the model. To further validate the model, we want to obtain data at other temperatures, inside and outside the 60-85 ^{o}C range. We recommend the parameter ranking and selection methods used in this study for other olefin polymerization models as we were able to estimate 53 out of 60 parameters to obtain good model predictions without overfitting the data. We anticipate that adding more data to our parameter estimation study in the future will result in additional estimable parameters and narrower confidence intervals for the estimable parameters.

The proposed model and its parameter estimates will be valuable for simulating new reactor conditions and for evaluating if the targeted MWD and CCD properties can be achieved with a particular catalyst system under feasible reactor conditions prior to pilot plant or commercial trials. Since lab-scale reactor tests usually cover wider ranges of temperature and 1-hexene over pilot plant, the proposed model may provide additional information, such as gels generation possibilities. A future study will incorporate pilot plant data into the model to obtain new parameter estimates. This would help fine-tune kinetic parameters for reactor property control once a promising catalyst system is identified and ready for scaling up to commercial scale reactors.

References

[1] A. Shamiri, M. H. Chakrabarti, S. Jahan, M. A. Hussain, W. Kaminsky, P. V. Aravind, W. A. Yehye, *Materials* **2014**, *7*, 5069.

[2] J. B. P. Soares, T. F. L. McKenna, *Polyolefin Reaction Engineering*, Wiley-VCH, Weinheim, Germany **2012**.

[3] W. Kaminsky, *Macromol. Chem. Phys.* **1996**, *197*, 3907.

[4] A. E. Hamielec, J. B. P. Soares, *Prog. Polym. Sci.* **1996**, *21*, 651.

[5] S. Mehdiabadi, J. B. P. Soares, J. Brinen, *Macromolecules* **2018**, *51*, 7061.

[6] T. Charoenpanich, S. Anantawaraskul, J. B. P. Soares, *Macromol. React. Eng.* **2016**, *10*, 215.

[7] D. J. Crowther, T. M. Boller, R. B. Pannell, J. M. Diop, W. Li (ExxonMobil Chemical Patents Inc.), US Patent 2021/11015002 B2, **2021**.

[8] D. E. Thompson, K. B. McAuley, P. J. McLellan, *Macromol. React. Eng.* **2007**, *1*, 523.

[9] D. E. Thompson, K. B. McAuley, P. J. McLellan, *Macromol. React. Eng.* **2010**, *4*, 73.

[10] R. A. Hutchinson, W. H. Ray, *J. Appl. Polym. Sci.* **1990**, *41*, 51.

[11] J. P. Aiello, Y. Jiang, J. A. Moebus, B. R. Greenhalgh, K. B. McAuley, *Macromol. Theory Simul.* **2021**, *30*, 2000079.

[12] J. A. Moebus, B. R. Greenhalgh, *Macromol. React. Eng.* **2018**, *72*, 1700072.

[13] S. Wu, K. A. P. McLean, T. J. Harris, K. B. McAuley, *Int. J. Adv. Mechatron. Syst.* **2011**, *3*, 188.

[14] K. Z. Yao, B. M. Shaw, B. Kou, K. B. McAuley, D. W. Bacon, *Polym. React. Eng.* **2003**, *11*, 563.

[15] D. E. Thompson, K. B. McAuley, P. J. McLellan, *Macromol. React. Eng.* **2009**, *3*, 160.

[16] S. Wu, K. B. McAuley, T. J. Harris, *Can. J. Chem. Eng.* **2011**, *89*, 148.

[17] S. Wu, K. B. McAuley, T. J. Harris, *Can. J. Chem. Eng.* **2011**, *89*, 325.

[18] K. A. P. McLean, K. B. McAuley, *Can. J. Chem. Eng.* **2012**, *90*, 351.

[19] B. Kou, K. B. McAuley, J. C. C. Hsu, D. W. Bacon, *Macromol. Mater. Eng.* **2005**, *290*, 537.

[20] Y. R. Zhao, K. B. McAuley, J. E. Puskas, *AlChE J.* **2015**, *61*, 253.

[21] R. Currie, M. W. Fowler, D. S. A. Simakov, *Chem. Eng. J.* **2019**, *372*, 1240.

[22] H. Karimi, B. Olayiwola, H. Farag, K. B. McAuley, *Can. J. Chem. Eng.* **2020**, *98*, 158.

[23] F. F. Liu, K. B. McAuley, *Macromol. React. Eng.* **2020**, *14*, 1900037.

[24] A. D. D. Vo, R. E. Spence, K. B. McAuley, *Macromol. Theory Simul.* **2021**, *30*, 2000061.

[25] B. T. Huang, N. S. Hayek, G. J. Sun, S. Mottaghi-Tabar, D. S. A. Simakov, O. M. Gazit, *Energy Fuels,* **2021**, *35*, 9589.

[26] M. Sen, A. J. Arguelles, S. D. Stamatis, S. Garcia-Munoz, S. Kolis, *React. Chem. Eng.* **2021**, *6*, 2092.

[27] K. Y. Choi, S. H. Tang, A. Sirohi, *Ind. Eng. Chem. Res.* **1997**, *36*, 1095.

[28] N. P. Khare, K. C. Seavey, Y. A. Liu, *Ind. Eng. Chem. Res.* **2002**, *41*, 5601.

[29] S. Y. Park, K. Y. Choi, K. H. Song, B. G. Jeong, *Macromolecules* **2003**, *36*, 4216.

[30] S. Y. Park, K. Y. Choi, *Macromol. Mater. Eng.* **2005**, *290*, 353.

[31] S. Y. Park, J. Lee, K. Y. Choi, *Macromol. React. Eng.* **2007**, *1*, 68.

[32] M. F. Bergstra, G. Weickert, G. B. Meier, *Macromol. React. Eng.* **2009**, *3*, 433.

[33] M. Ahmadi, M. Nekoomanesh, H. Arabi, *Macromol. React. Eng.* **2010**, *4*, 135.

[34] K. Chen, S. Mehdiabadi, J. B. P. Soares, *Macromol. React. Eng.* **2016**, *10*, 551.

[35] S. Mehdiabadi, J. B. P. Soares, *Macromolecules* **2016**, *49*, 2448.

[36] V. Touloupidis, A. Albrecht, J. B. P. Soares, *Macromol. React. Eng.* **2018**, *12*, 1700056.

[37] S. Saadat, J. B. P. Soares, P. J. DesLauriers, J. S. Fodor, *Macromol. React. Eng.* **2019**, *14*, 1900032.

[38] X.-P. Cheng, L.-F. Feng, X.-P. Gu, X. Chen, Z.-G. Liu, K. B. McAuley, *AlChE J.* **2020**, *66*, e16784.

[39] Z. G. Xu, S. Chakravarti, W. H. Ray, *J. Appl. Polym. Sci.* **2001**, *80*, 81.

[40] Chakravarti, S. W. H. Ray, *J. Appl. Polym. Sci.* **2001**, *80*, 1096.

[41] S. Chakravarti, W. H. Ray, S. X. Zhang, *J. Appl. Polym. Sci.* **2001**, *81*, 1451.

[42] M. Ahmadi, M. Nekoomanesh, R. Jamjah, G. Zohuri, H. Arabi, *Macromol. Theory. Simul.* **2007**, *16*, 557.

[43] S. Mehdiabadi, J. B. P. Soares, *Macromol. Chem. Phys.* **2013**, *214, 246*.

[44] A. L. T. Brandão, A. L. Alberton, J. C. Pinto, J. B. P. Soares, *Macromol. Theory Simul.* **2017**, *26*, 1600059.

[45] A. Caldera, J. B. P. Soares, P. J. DesLauriers, J. S. Fodor, *J. Catal.* **2019**, *375*, 140.

[46] N. Sharma, Y. A. Liu, *Ind. Eng. Chem. Res.* **2019**, *58*, 14209.

[47] D. J. Pritchard, D. W. Bacon, *Chem. Eng. Sci.* **1975**, *30*, 567.

[48] M. Schwaab, L. P. Lemos, J. C. Pinto, *Chem. Eng. Sci.* **2008**, *63*, 2895.

[49] K. R. Chen, S. Mehdiabadi, B. P. Liu, J. B. P. Soares, *Macromol. React. Eng.* **2016**, *10*, 206.

[50] T. Y. Xie, K. B. McAuley, J. C. C. Hsu, D. W. Bacon, *Ind. Eng. Chem. Res.* **1994**, *33*, 449.

[51] D. Bonvin, C. Georgakis, C. C. Pantelides, M. Barolo, M. A. Grover, D. Rodrigues, R. Schneider, D. Dochain, *Ind. Eng. Chem. Res.* **2016**, *55*, 6891.

[52] A. Buso, M. Giomo, *Numerical Simulations of Physical and Engineering Processes*, IntechOpen, **2011**

[53] A. G. Mattos Neto, M. F. Freitas, M. Nele, J. C. Pinto, *Ind. Eng. Chem. Res.* **2005**, *44*, 2697.

[54] S. Floyd, T. Heiskanen, T. W. Taylor, G. E. Mann, W. H. Ray, *J. Appl. Polym. Sci.* **1987**, *33*, 1021.

[55] K. B. McAuley, J. F. MacGregor, A. E. Hamielec, *AlChEJ.* **1990**, *36*, 837.

[56] J. B. P. Soares, *Macromol. React. Eng.* **2013**, *8*, 235.

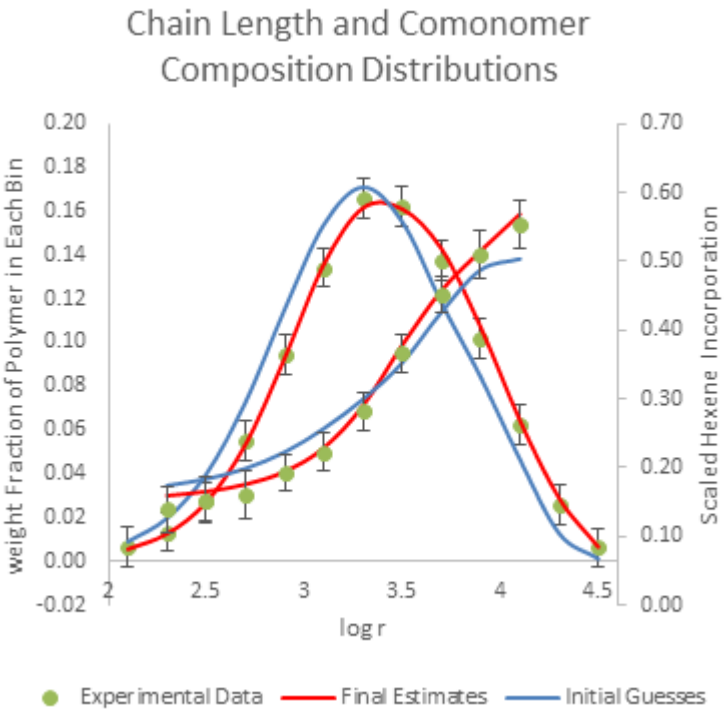

Mathematical models with estimated kinetic rate parameters are required to scale up new polyethylene products and optimize commercial reactor performance. A kinetic model that describes lab-scale gas-phase ethylene/1-hexene copolymerization using a 3-site hafnocene catalyst at different temperatures is developed. Kinetic rate constants and activation energies are estimated from joint molecular weight and comonomer composition distribution data.